AD_____

Award Number: DAMD17-02-2-0011

TITLE: Structural Studies on Intact Clostridium Botulinum Neurotoxins Complexed with Inhibitors Leading to Drug Design

PRINCIPAL INVESTIGATOR: Subramanyam Swaminathan, Ph.D.

CONTRACTING ORGANIZATION: Brookhaven National Laboratory
Upton, New York 11973

REPORT DATE: February 2004

TYPE OF REPORT: Annual

PREPARED FOR: U.S. Army Medical Research and Materiel Command
Fort Detrick, Maryland 21702-5012

REPORT DOCUMENTATION PAGE

Form Approved
OMB No. 074-0188

1. AGENCY USE ONLY (Leave blank)	2. REPORT DATE	3. REPORT TYPE AND DATES COVERED
	February 2004	Annual (28 Jan 2003 - 27 Jan 2004)

4. TITLE AND SUBTITLE
Structural Studies on Intact Clostridium Botulinum Neurotoxins Complexed with Inhibitors Leading to Drug Design

5. FUNDING NUMBERS
DAMD17-02-2-0011

6. AUTHOR(S)
Subramanyam Swaminathan, Ph.D.

7. PERFORMING ORGANIZATION NAME(S) AND ADDRESS(ES)
Brookhaven National Laboratory
Upton, New York 11973

E-Mail: swami@bnl.gov

8. PERFORMING ORGANIZATION REPORT NUMBER

9. SPONSORING / MONITORING AGENCY NAME(S) AND ADDRESS(ES)
U.S. Army Medical Research and Materiel Command
Fort Detrick, Maryland 21702-5012

10. SPONSORING / MONITORING AGENCY REPORT NUMBER

11. SUPPLEMENTARY NOTES
Original contains color plates: All DTIC reproductions will be in black and white.

12a. DISTRIBUTION / AVAILABILITY STATEMENT
Approved for Public Release; Distribution Unlimited

12b. DISTRIBUTION CODE

13. ABSTRACT (Maximum 200 Words)
In this second annual report we present our progress on three different areas. We are working on intact BoNT/B to identify small molecules that could be used to block the toxic activity. In this respect, we have discovered that two calcium ions are bound to BoNT/B and that at least one of them plays an important role in the translocation of the catalytic domain into the cytosol. We propose that this calcium ion site could be targeted by calcium specific chelators to block translocation. As for the ganglioside binding site as a target, we are workin with both intact BoNT/B and structurally similar C fragment of tetanus neurotoxin. We have identified two molecules that might compete with ganglioside for binding which could potentially be used as inhibitor. One of our Statements Of Work is to work with Clostridium botulinum neurotoxin E. Since the diffraction quality of intact toxin is poor, it is difficult to use the intact toxin for inhibitor study via x-ray crystallography. We are using BoNT/E light chain to this inhibitor study and have determined the crystal structure of BoNT/E light.

14. SUBJECT TERMS
Clostridium, botulinum, neurotoxin, zinc chelators, inhibitors, macromolecular crystallography, 3D structure

15. NUMBER OF PAGES
28

16. PRICE CODE

17. SECURITY CLASSIFICATION OF REPORT	18. SECURITY CLASSIFICATION OF THIS PAGE	19. SECURITY CLASSIFICATION OF ABSTRACT	20. LIMITATION OF ABSTRACT
Unclassified	Unclassified	Unclassified	Unlimited

Table of Contents

Structural Studies on Intact *Clostridium botulinum* Neurotoxins Complexed with Inhibitors Leading to Drug Design
Annual Report for the Period ending January 2004

Introduction

The major goal of this project is to identify small molecules that will inhibit the toxicity of botulinum neurotoxins (BoNTs). The two sites that we target are the receptor binding site and the catalytic activity site. Since gangliosides from neuronal cells attach to the binding site in the first step of toxicity, we are trying sugar or drug molecules that will mimic the ganglioside sugar groups to block the site. Since C. neurotoxins are zinc endopeptidases, we also are trying small molecule zinc chelators that will block the active site zinc from being available for catalytic activity. The general approach is to study the crystal structure of the toxin in complex with a potential inhibitor via x-ray crystallography and then analyze the interactions between the inhibitor and the protein. However, this approach will work best when we can get high-resolution data. Accordingly, we have made a slight change in our approach this year. While we are still continuing our study with intact BoNT/B, we have started to work with the catalytic domain of BoNT/E since intact BoNT/E does not diffract to high resolution. In addition we are continuing to understand the structure – function relationship to identify other regions in the neurotoxin which can be targeted for drug design.

Body

(1) Structural analysis of C. neurotoxins in complex with molecules binding to the C-terminal domain of C. neurotoxin

Botulinum neurotoxins and tetanus neurotoxin share significant sequence homology and are therefore expected to have similar three-dimensional structures. The experimental models of the C-fragment of tetanus toxin and the C-terminal domain have similar structure except for the loop regions. The cavity at the sugar-binding site which was defined in BoNT/B is similar to the cavity present in the C-fragment of tetanus toxin

(rTTC). Based on this it is reasonable to hypothesize that any molecule that binds to tetanus toxin will also bind to other botulinum toxins. We have proved this in a few cases. Here we are reporting our studies with the C-fragment of tetanus toxin with disialyllactose and a tripeptide which has been identified by docking studies. Disialyllactose is particularly interesting since it forms one branch of the sugar moiety of GT1b; also it is the sugar moiety of GD3.

(a) RTTC in complex with disialyllactose

Crystals of rTTC where obtained as described by Umland et al. (1). Crystals of rTTC were soaked in the mother liquor containing 50 mM disialyllactose which was determined from preliminary experiments. Crystals were soaked overnight in the mother liquor containing the sugar and then flash frozen in liquid nitrogen using 10 % glycerol. X-ray diffraction data were collected at X12C beamline of the NSLS, Brookhaven National Laboratory. Molecular replacement using AMORE was used to solve the structure (2). The crystal structure of the rTTC (3), was used as a search model. After initial rigid body refinement structure was refined with CNS (4) and the model was examined with O (5). The model was complete except 940-948 region. This region is not well defined in the electron density map. A σA-weighted Fo-Fc map was calculated with refined models. Initial map showed clear density for the two silaic acid molecules and Gal residue. Glc was fitted after two cycles of refinement. O was used to build the molecule into the electron density. A preliminary Ribbons drawing with the disialyllactose is shown in Figure 1a. The structure has been refined and a manuscript is being submitted for publication.

(b) rTTC and TRY-GLU-TRP (YEW) complex

Soaking conditions were similar to that of disialyllactose. Data were collected under similar conditions. The structure was determined using AMORE. Ribbons representation of rTTC with YEW is shown in Figure 1b. The structure has been refined and the results will be published soon.

(a) (b)

Figure 1: (a) Ribbons representation of rTTC with disialyllactose shown as ball and stick model. Disialyllactose binds in a region adjacent to sialyllactose in BoNT/B. (b) rTTC shown in ribbons representation. YEW is shown as sphere model. It occupies the same binding site as disialyllactose

(2) Calcium ion plays a role in the translocation

In the course of high-resolution structure determination of BoNT/B, we have identified two calcium ions bound to the molecule. Though many zinc endopeptidases have calcium ions bound to them, this is the first time calcium ions have been found in C. neurotoxins. In thermolysin and other zinc endopeptidases, the calcium is attributed to stabilize the conformation of the protein. However, in our study we have shown by biochemical methods that calcium ions play a role in the translocation of the catalytic domain into the cytosol. This may give an additional target for inhibiting the toxicity of C. neurotoxins. If metal chelators specific to calcium could be used, the translocation could be blocked. A paper describing these results have been accepted by Biochemistry for publication and a PDF file is attached in the appendix (Appendix 1). In addition to discussion on calcium ions, this paper also describes our experiments and apo toxin and the effect pH variation on C. neurotoxin.

(3) Studies with C. neurotoxin type E catalytic domain

(a) Cloning, expression and purification of BoNT/E catalytic domain

While Clostridium botulinum neurotoxin Type B (BoNT/B) crystals diffract well and it is possible to collect high-resolution data, the same is not true with BoNT/E holotoxin. In order study the interaction between the active site and the inhibitor, we need high-resolution data. In the case of BoNT/E we have decided to follow the approach of studying only the catalytic domain with the inhibitors. However, intact BoNT/E will be tried simultaneously.

An ampicillin resistant inducible T5-promoter expression vector pBN17, encoding a full length (1263 bp) of botulinum neurotoxin E light chain (BoNT/E-LC) region fused to a C-terminal 6x His tag, was obtained from Dr. Thomas Binz, Medizinische Hochschule Hanover, Germany. It was transformed and expressed in the BL21 cells but the protein yield was less than 0.5 mg per liter of culture medium. Our major goal is to crystallize the catalytic domain of BoNT/E and large-scale crystallization trials typically require milligram amounts of a highly pure, soluble protein as starting material. In an attempt to get a higher yield the gene was amplified by PCR and then was cloned into pET-9c which is a bacteriophage T7-RNA polymerase promoter vector system. The T7-RNA polymerase is highly capable of transcribing almost any DNA linked to a T7 promoter (7). The aim was to over-express the full-length light chain and maintain its catalytic activity.

The protein was over-expressed in BL21 (DE3) cells and the protein was purified in a two-step process – first with nickel column and then with a sizing column. This yielded 98% pure protein in enough quantity for crystallization. We could get about 30 mg of BoNT/E light chain for 1 liter of culture medium. The catalytic activity was checked with SNAP-25 and we find the protein is highly active. To the best of our knowledge, this is the first time such a high yield of active protein has been obtained. A paper describing these results has been published in Protein Expression and Purification and a PDF file is attached as appendix (Appendix 2).

(b) Crystal structure of the catalytic domain of BoNT/E

We have obtained crystals of BoNT/E light chain and Single-wavelength anomalous dispersion (SAD) data were collected using zinc as anomalous scatterer at the National Synchrotron Light Source at Brookhaven National Laboratory. The crystals belong to the orthorhombic space group with cell dimensions a = 88.4, b = 146.5 and c = 83.2 Å with two molecules per asymmetric unit. This is the first time the crystal structure of a molecule of this size (~50 kDa) has been determined using the anomalous signal from one zinc atom per molecule. The structure determination and refinement are complete. Interestingly, the molecules exist as a dimer in the crystal structure with the active sites of both molecules exposed to the solvent (Fig. 2). This crystal will be used for soaking experiments to identify inhibitors for BoNT/E. We will be using combinatorial chemistry, virtual screening, small molecule docking and x-ray crystallography to identify such molecules

Figure 2. Ribbons representation of BoNT/E-LC dimer. The two monomers are in green and blue. The active site zinc and the coordinating protein residues are in ball and stick model.

Key Research Accomplishments

- Two small molecules have been identified which may help in designing molecules to block gangliosides binding to C. neurotoxin.
- The same molecules also provide a model for ganglioside binding to neurotoxins.
- For the first time calcium ions have been discovered to bind to C. neurotoxin. This provides an additional target for blocking toxic activity.
- A method has been developed to obtain large quantities of BoNT/E light chain for X-ray crystallographic work.
- Crystal structure of BoNT/E light chain can now be used for identifying inhibitors for BoNT/E.

Reportable outcomes

1. A poster was presented at the American Crystallographic Association meeting. Crystal structure of the binding domain of tetanus toxin: disialyllactose complex. J. Seetharaman, S. Eswaramoorthy, D. Kumaran and S. Swaminathan. (Abstract # P168) ACA 2003 Annual meeting, Cincinnati, Ohio, USA.

2. A platform presentation was given by S. Swaminathan at the Interagency Botulinum Research Consortium Committee meeting held in October, 2003 at Atlanta, Ga.

3. Presented an invited talk at the University of Miami Medical School, Miami, April 2003.

4. Rakhi Agarwal, S. Eswaramoorthy, D. Kumaran, J. Dunn and S. Swaminathan. Cloning high level expression purification and crystallization of the full length Clstridium botulinum neurotoxin type E light chain. *Protein Expression & Purification*, 2004, **34**, 95-102.

5. S. Eswaramoorthy, D. Kumaran, J. Keller and S. Swaminathan. "Role of Metals in the Biological Activity of Clostridium botulinum Neurotoxins", *Biochemistry*, 2004, **43(8)**, 2209 – 2216.

Conclusions

In our studies we have shown that the ganglioside binding site could be blocked with small molecules and could be used as inhibitor molecules to block botulinum toxicity. We have also shown that calcium is bound to the neurotoxin and plays a role in the translocation mechanism and this could perhaps be used as a target for blocking toxicity. We have cloned and expressed full length BoNT/E light chain and that it is active in vitro and could be used for designing inhibitors.

Plans for the next quarter:

Virtual screening and x-ray crystallography methods will be combined to identify small molecule inhibitors for BoNT/E. Also structural work on BoNT/B-inhibitor complex will be continued.

Personnel in the Project

1. S. Swaminathan (PI)	Scientist	20% effort
2. S. Eswaramoorthy	Associate Scientist	50% EFFORT
3. R. Agarwal	Research Associate	100% effort

Reference:

1. Umland, T. C., Wingert, L., Swaminathan, S., Schmidt, J. J., and Sax, M. (1998) *Acta Crystallographica* **D54**, 273-275
2. Navaza, J., and Saludjian, P. (1997) *Methods Enzymol.* **276**, 581-594
3. Umland, T. C., Wingert, L. M., Swaminathan, S., Furey, W. F., Schmidt, J. J., and Sax, M. (1997) *Nature Struct. Biol.* **4**, 788-792
4. Brunger, A. T., Adams, P. D., Clore, G. M., Delano, W. L., Gros, P., Grosse-Kunstleve, R. W., Jiang, J. S., Kuszwewski, J., Nilges, M., Pannu, N. S., Read, R. J., Rice, L. M., Somonsom, T., and Warren, G. L. (1998) *Acta Crystallogr.* **D54**, 905-921
5. Jones, T. A., Zou, J., Cowtan, S., and Kjeldgaard, M. (1991) *Acta Crystallogr.* **A47**, 110 - 119
6. Swaminathan, S., and Eswaramoorthy, S. (2000) *Nat. Struct. Biol.* **7**, 693-699

7. Studier, F. W., Rosenberg, A. H., Dunn, J. J., and Dubendorff, J. W. (1990) *Methods Enzymol.* **185**, 60-89

Biochemistry **2004,** *43,* 2209−2216

Role of Metals in the Biological Activity of *Clostridium botulinum* Neurotoxins[†,‡]

Subramaniam Eswaramoorthy,[§] Desigan Kumaran,[§] James Keller,[∥] and Subramanyam Swaminathan*[,§]

Biology Department, Brookhaven National Laboratory, Upton, New York 11973, and Laboratory of Bacterial Toxins, Food and Drug Administration, Bethesda, Maryland 20892

Received October 13, 2003; Revised Manuscript Received December 22, 2003

ABSTRACT: *Clostridium botulinum* neurotoxins are the most potent toxins to humans and cause paralysis by blocking neurotransmitter release at the presynaptic nerve terminals. The toxicity involves four steps, viz., binding to neuronal cells, internalization, translocation, and catalytic activity. While the catalytic activity is a zinc endopeptidase activity on the SNARE complex proteins, the translocation is believed to be a pH-dependent process allowing the translocation domain to change its conformation to penetrate the endosomal membrane. Here, we report the crystal structures of botulinum neurotoxin type B at various pHs and of an apo form of the neurotoxin, and discuss the role of metal ions and the effect of pH variation in the biological activity. Except for the perturbation of a few side chains, the conformation of the catalytic domain is unchanged in the zinc-depleted apotoxin, suggesting that zinc's role is catalytic. We have also identified two calcium ions in the molecule and present biochemical evidence to show that they play a role in the translocation of the light chain through the membrane.

Clostridium neurotoxins comprise the seven antigenically distinct neurotoxins (BoNT/A-G)[1] produced by *Clostridium botulinum* and tetanus neurotoxin produced by *Clostridium tetani*. Active neurotoxins are two-chain molecules, a heavy chain (HC, 100 kDa) and a light chain (LC, 50 kDa) held together by a disulfide bond (*1*). Botulinum neurotoxins act on the peripheral nervous system and inhibit the release of acetylcholine at the neuromuscular junction (*2*). Tetanus toxin acts on the central nervous system and inhibits the release of glycine and γ-aminobutyric acid (*3*). They all share significant sequence homology and functional similarity and are expected to have similar three-dimensional structures. *C. botulinum* neurotoxins follow a four-step process of toxicity (*4*−*6*). The C-terminal half of the HC binds to the presynaptic membrane via gangliosides and to a second protein receptor, and then the toxin is internalized by receptor-mediated endocytosis. The N-terminal half of the HC helps in translocating the LC into the cytosol where the latter cleaves one of the three target proteins at specific peptide bonds, thus inhibiting formation of the SNARE complex, which is necessary for docking and fusion of vesicles to membranes. This in turn blocks the release of neurotransmitters and causes flaccid (botulinum toxins) or spastic paralysis (tetanus toxin). The LCs of all neurotoxins contain a conserved zinc-binding motif (HExxH+E), and accordingly, at least one zinc atom is present per molecule (*7*). The catalytic activity is a zinc endopeptidase activity, and therefore, the presence of zinc is required for activity. Though they have similar functions and sequences, the target protein and the scissile bonds are specific for each neurotoxin. BoNT/A, -E, and -C1 cleave synaptosomal-associated protein (SNAP-25) at different peptide bonds. BoNT/B, -D, -F, and -G and tetanus toxin cleave vesicle-associated membrane protein (VAMP). BoNT/C also cleaves syntaxin (*7*−*15*).

The role of zinc in *Clostridium* neurotoxins has been studied extensively by biochemical and biophysical methods. A zinc atom is present in many proteins, and its role is to maintain the structural integrity, the functional integrity, or both (*16*−*18*). There are conflicting opinions about the role of zinc in *Clostridium* neurotoxins. It has been shown to be functional in the case of BoNT/B and tetanus toxin since the catalytic activity that was lost upon the removal of zinc was regained when it was introduced again into the protein, suggesting that there is no structural change when zinc is removed or reintroduced (*7*, *19*, *20*). In the case of intact BoNT/A, the activity could not be restored by reintroducing the zinc atom. This led to the conclusion that while the removal of zinc is reversible, the activity is irreversibly lost presumably due to a change in the tertiary structure (*21*). This was supported by circular dichroism and spectroscopic studies. However, the activity could be restored in the BoNTA light chain, though to a lesser extent (*22*). Simpson et al. (*23*) have recently shown that the role of zinc is only catalytic. However, no X-ray structure of the zinc-depleted protein has been available until now for comparing the apo- and holotoxin conformations directly. Here, we present the

[†] Research supported by the Chemical and Biological Non-proliferation Program (NN20) of the U.S. Department of Energy and the U.S. Army Medical Research Acquisition Activity (Award DAMD17-02-2-0011) under DOE Prime Contract DE-AC02-98CH10886 with Brookhaven National Laboratory.

[‡] The coordinates for the structures have been deposited in the Protein Data Bank as entries 1S0B, 1S0C, 1S0D, 1S0E, 1S0F, and 1S0G.

* To whom correspondence should be addressed. E-mail: swami@bnl.gov. Telephone: (631) 344-3187. Fax: (631) 344-3407.

[§] Brookhaven National Laboratory.

[∥] Food and Drug Administration.

[1] Abbreviations: BoNT, botulinum neurotoxin; HC, heavy chain; LC, light chain; SNARE, soluble NSF accessory protein receptors; SNAP-25, synaptosome-associated protein of 25 kDa; VAMP, vesicle-associated membrane protein; DTT, dithiothreitol; EDTA, ethylenediaminetetraacetate; TPEN, *N,N,N′,N′*-tetrakis(2-pyridylmethyl)ethylenediamine; PMSF, phenylmethanesulfonyl fluoride; BAPTA, 1,2-bis(2-aminophenoxy)ethane-*N,N,N′,N′*-tetraacetic acid; HEPES, *N*-(2-hydroxyethyl)piperazine-*N′*-2-ethanesulfonic acid.

10.1021/bi035844k CCC: $27.50
Published on Web 02/06/2004

first three-dimensional structure of an apo *Clostridium* neurotoxin determined by X-ray diffraction.

The process of translocation of the LC into the cytosol is still a puzzle. The translocation domain probably changes its conformation due to the pH change in the endosome which allows it to insert itself into the endosomal membrane and translocate the LC into the cytosol (*5*, *24*). We have determined the crystal structure of BoNT/B at various pH values ranging from 4 to 7 and show that there is no conformational change at the putative transmembrane region, at least in the crystal structures. There may be other factors, yet unknown, involved in the translocation (*25*). We have identified two calcium ions bound to the toxin molecule which play a role in the translocation of the catalytic domain.

In this report, we present the results from the crystal structure analysis of the apotoxin and BoNT/B crystallized at various pHs and also provide biochemical evidence which shows that calcium is required for translocation of the neurotoxin into the cytosol.

EXPERIMENTAL PROCEDURES

Reagents. Trypsin, soybean trypsin inhibitor, *N,N,N′,N′*-tetrakis(2-pyridylmethyl)ethylenediamine (TPEN), phenylmethanesulfonyl fluoride (PMSF), 1,2-bis(2-aminophenoxy)-ethane-*N,N,N′,N′*-tetraacetic acid (BAPTA), the membrane-permeable BAPTA-AM, and dithiothreitol were from Sigma Chemical Co. (St. Louis, MO). SDS−PAGE and Western blotting supplies were from Bio-Rad (Hercules, CA).

Toxin Preparation. In the case of cell culture experiments, BoNT/A and -B were obtained from Wako Chemicals (Richmond, VA). According to the manufacturer's instructions, BoNT/B [1 mg/mL in 0.2 M NaCl and 50 mM NaOAc (pH 6.0)] was treated with trypsin (0.2 mg/mL) at 37 °C for 0.5 h. Trypsin was inhibited by addition of soybean trypsin inhibitor (0.5 mg/mL). Both serotypes were aliquoted and frozen at −20 °C. The clone, LC-pET30 with two six-histidine tags and one S-tag, for the BoNT/A light chain was a gift from R. Balhorn. It was expressed and purified in Swaminathan's laboratory as described previously (*26*). BoNT/B for crystallization was purchased from Metabiologics (Madison, WI).

Testing BoNT Action. Cultured spinal cord neurons were prepared from E12 mouse embryos and plated onto 35 mm dishes at a density of 1×10^6 cells. Cultures were maintained in MEM medium containing 5% horse serum (*27*−*29*) and fed with half-medium changes twice per week. Because Ca^{2+} is required for many cell functions, the toxin (BoNT/A and -B at 0.5 and 2 nM, respectively) was applied to cells in the presence of 2 mM Ca^{2+} to allow normal toxin binding and endocytosis. Four minutes after the toxin had been added, cultures were washed to remove unbound toxin and then were incubated for 2.5 h at 37 °C. The Ca^{2+}-specific chelator BAPTA-AM was prepared as a 50 mM stock solution in DMSO. This was diluted into Ca^{2+}-free MEM and applied to cultures immediately after toxin washout. The absence of Ca^{2+} in the extracellular medium after toxin application did not alter intracellular BoNT activity. To directly test toxin activity on SNARE substrates, some cultures were lysed using 0.6% Triton, 0.5 mM PMSF, 1 mM DTT, and 25 mM HEPES (pH 7.2). The lysate was incubated on ice for 1 h to allow PMSF to degrade prior to toxin addition. Lysate/toxin mixtures were incubated at room temperature for 3 h.

SDS−PAGE and Western Blot Analysis. We prepared samples from neuronal cultures or lysates for SDS−PAGE by dissolving them in 2% SDS and 0.5% mercaptoethanol and boiling for 4 min. Proteins were separated on 15% acrylamide gels (*30*) and transferred to a PVDF membrane. Western blotting utilized antibodies to SNARE complex proteins: the anti-SNAP-25 antibody was from Sternberger Monoclonals (Lutherville, MD), anti-Synaptobrevin-2 from Synaptic Systems, and anti-syntaxin from Sigma Chemical Co. A secondary antibody was conjugated to horseradish peroxidase and visualized using ECL-Plus chemiluminescent substrate (Amersham Bioscience, Piscataway, NJ). Blot images were obtained by scanning with the STORM 860 fluorescent detector and ImageQuant software (Molecular Dynamics).

Preparation of the Protein for Crystallization. BoNT/B was supplied as a precipitate in 50% ammonium sulfate. This was spun at 5000 rpm in a refrigerated microcentrifuge, and the supernatant was discarded. The precipitate was dissolved in 50 mM HEPES, 100 mM NaCl, and 10 mM dithiothreitol (DTT) at pH 7.0. DTT was used since the BoNT endopeptidase activity is expressed only after the disulfide bond is reduced (*31*). Also, because the protein is supplied as a precipitate in ammonium sulfate, a sulfate ion was found to be present in the catalytic site (*32*). The protein was dialyzed against 100 mM NaCl, 50 mM HEPES, and 10 mM dithiothreitol at pH 7.0 overnight in two steps. Then 80 mM barium acetate was added to the dialysate to remove the sulfate ion bound in the catalytic site and dialyzed twice more. The final dialysis was carried out without barium acetate.

Preparation of the Apoprotein. The protein (1 mg/mL) was prepared as described above, but metal-free HPLC-grade water was used throughout. The protein was then treated with ethylenediaminetetraacetate (EDTA) to a final concentration of 15 mM and incubated for 1 h at 37 °C. This was again extensively dialyzed against 50 mM HEPES, 100 mM NaCl, and 10 mM DTT at pH 7.0 to remove EDTA and the zinc−EDTA complex (*21*).

Crystallization. The crystallization condition for both apo- and holoneurotoxins is as described but under a reducing condition (*33*). In the case of the apoprotein, the reagents were prepared with HPLC-grade water. For the holotoxin, crystallization was carried out at pH 5.0 using appropriate buffer. To determine crystal structures at other pH values, the pH of the mother liquor was slowly titrated with appropriate buffers (sodium citrate for pH <5.5 and HEPES for pH >5.5), allowing enough time (6 h for each change) for the crystals to equilibrate with the mother liquor. The crystals were monitored periodically to check for any physical damage. Crystals were obtained at pH 4.0, 5.0, 5.5, 6.0, and 7.0.

Data Collection. Data were collected at liquid nitrogen temperature at X12C and X25 beamlines of the National Synchrotron Light Source, Brookhaven National Laboratory, with a Brandeis CCD-based B1 or B4 detector. An oscillation range of 1° was used for each data frame, and data corresponding to 200° in ϕ were collected with a crystal to detector distance of 100 mm (200 mm at X25) and a λ of 1.00 Å. Data were reduced with DENZO and SCALEPACK (*34*). Data collection statistics are given in Table 1.

Table 1: Crystal Data and Refinement Statistics[a]

	pH 4.0	pH 5.0	pH 5.5	pH 6.0	pH 7.0	apo
			Crystal Data			
resolution (Å)	2.0	2.2	2.2	1.9	2.3	2.6
total no. of reflections	284241	295339	275095	368649	254516	172822
no. of unique reflections	97573	81173	78587	118562	64761	49302
completeness (%)[b]	89.1 (69.4)	99.7 (98.4)	94.3 (74.8)	92.8 (55.4)	89.8 (51.9)	99.7 (97.7)
R_{sym}[c]	0.059 (0.218)	0.079 (0.310)	0.067 (0.397)	0.048 (0.308)	0.084 (0.497)	0.055 (0.166)
			Refinement Parameters			
resolution (Å)	50.0−2.0	50.0−2.2	50.0−2.2	50.0−1.9	50.0−2.3	50.0−2.6
no. of reflections	94427	77445	70860	112138	58061	48272
R[d]	0.204	0.204	0.223	0.206	0.226	0.210
R_{free}[e]	0.234	0.240	0.273	0.235	0.287	0.265
no. of atoms						
protein	10587	10587	10587	10587	10430	10594
Zn^{2+}	−	1	1	1	1	−
Ca^{2+}	2	2	2	2	2	−
no. of water molecules	1034	582	547	857	428	379
rmsd						
bond lengths (Å)	0.006	0.006	0.007	0.006	0.007	0.007
bond angles (deg)	1.21	1.23	1.26	1.21	1.28	1.27
% residues in the most favored region of the $\phi-\psi$ plot[f]	88.4 (11.0)	88.1 (11.0)	87.6 (11.5)	88.1 (11.2)	83.2 (15.4)	86.5 (12.7)

[a] Cell parameters at pH 6: $a = 76.05$ Å, $b = 122.91$ Å, $c = 95.43$ Å, and $\beta = 113.1°$. Cell parameters for other pHs and for the apotoxin agree within experimental error. [b] Values for the outermost shells are given in parentheses. [c] $R_{sym} = \sum_h\sum_i|I_i(h) - \langle I(h)\rangle|/\sum_h\sum_i|I_i(h)|$, where $I_i(h)$ is the intensity measurement for reflection h and $\langle I(h)\rangle$ is the mean intensity for this reflection. [d] $R = \sum_i||F_{i,obs}| - k|F_{i,cal}||/\sum_i|F_{i,obs}|$. [e] Approximately 2% of the total reflections were used for R_{free} calculations. [f] Percentage of residues in the additional allowed region given in parentheses.

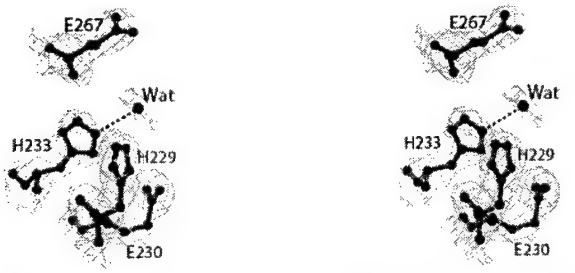

FIGURE 1: SigmaA-weighted $2F_o - F_c$ map at the active site of the apotoxin. Contours are drawn at the 1σ level. There is no residual density corresponding to the original zinc site. The residual density close to the zinc site is due to water molecules. The coordination with Glu267 is lost. There is a water molecule near the original zinc site which may be disordered. This figure was prepared with Molscript (*52*).

Structure Determination. Initial model coordinates were obtained from Protein Data Bank entry 1epw. After initial rigid body refinement, the structures were refined with CNS (*35*). Adjustments of the original model were done with O (*36*) against a composite omit map to remove model bias. The protein model is complete except for residues 440−442, which are in the proteolytic site. In the case of the apoprotein, the sigmaA-weighted $2F_o - F_c$ map showed no density at the zinc site, confirming the absence of zinc (Figure 1) (*37*). The model was further refined with water molecules and metals (if present) included. Refinement statistics are included in Table 1. Structures were validated with PROCHECK (*38*), and the percentages of residues in the most favored region of the Ramachandran plot are given in Table 1.

RESULTS AND DISCUSSION

Structure of BoNT/B at pH 4, 5, 5.5, 6, and 7. The crystal structure of BoNT/B was determined under various (pH) conditions. A Ribbons representation of the molecule is given in Figure 3. The BoNT molecule consists of three functional domains which are the binding, translocation, and catalytic domains (left to right in Figure 3). The translocation domain consists mainly of two long helices, and the catalytic domain contains a zinc ion. While the binding domain is presumably invariant to pH variation, the translocation domain is supposed to undergo conformational variation to expose the hydrophobic residues to the membrane bilayer to allow channel formation for the translocation of the LC into the cytosol. The size of the pore formed by the BoNT/B HC has been estimated to be ~8−15 Å (*25*, *39*), and it is not clear how a 50 kDa domain could escape through it without completely unfolding. It is possible that the light chain completely unfolds at low pH, threads through the pore, and then refolds in the cytosol before attacking its target (*40*). However, there may be other factors involved in the change of conformation. This study is focused on only the effect of pH variation on the conformation of the protein.

Conformation of the Translocation Domain versus pH. Theoretical predictions about the transmembrane region based on hydropathy analysis concluded that the region of residues 637−668 for BoNT/B would be the transmembrane region and could adopt a helical conformation (*41*). However, in the structural analysis of BoNT/B carried out at pH 6.0, this region is not all helical. While residues 638−645 adopt a helical conformation and are in the middle of the molecule, the rest is in an extended conformation. This is similar to the BoNT/A structure which was determined at pH 7.0 (*42*). In BoNT/A, it is suggested that two histidines in the translocation domain (residues 551 and 560) might titrate during the reduction of the pH in the endosome and help in changing the conformation. However, no histidine is present in the translocation domain of BoNT/B to induce conformational change by the same mechanism. This prompted us to determine the structure at lower pH values. Figure 4 shows the superposition of the putative transmembrane region at various pHs. There is no change in the conformation in this

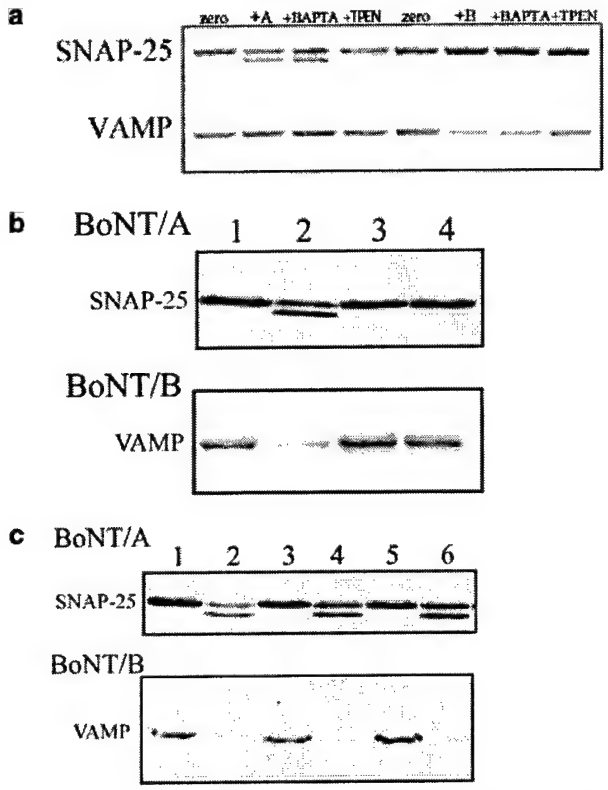

FIGURE 2: (a) Neuronal lysate treated with BoNT and chelators. Lysates were prepared as described in Experimental Procedures and treated with 0.1 mM BAPTA or TPEN as indicated. Reactions were initiated by addition of BoNT/A (10 nM) or BoNT/B (20 nM) light chains and then were stopped 3 h later. Densitometric analysis shows that each toxin cleaved approximately half of the SNARE protein substrate. BAPTA had no noticeable effect, whereas TPEN completely inhibited both, indicating that BAPTA could not chelate Zn^{2+} from the toxin light chains. (b) Living neurons treated with BoNT and chelators. Neuronal cultures were treated with BoNT/A (0.5 nM) or BoNT/B (2 nM). Some cultures were simultaneously treated with BAPTA-AM (80 μM) or TPEN (20 μM): lane 1, untreated; lane 2, BoNT only; lane 3, BAPTA-AM; and lane 4, TPEN. Western blot results show that both chelators inhibit intracellular BoNT activity. (c) Restoration of intracellular BoNT activity following chelator inhibition. Cultures were treated with BoNT as described for panel b except in some cases excess Ca^{2+} or Zn^{2+} was added to cultures: lane 1, untreated; lane 2, BoNT only; lane 3, BoNT and BAPTA-AM; lane 4, BoNT, BAPTA-AM, and 0.1 mM Ca^{2+}; lane 5, BoNT and TPEN; and lane 6, BoNT, TPEN, and 0.1 mM Zn^{2+}. Toxin inhibition by BAPTA-AM is reversed by free Ca^{2+}. Since BAPTA does not inhibit the catalytic activity of BoNT (a), Ca^{2+} probably has a direct role in entry of the toxin into the neuronal cytosol.

region as the pH of the crystal is varied. Though it takes an extended conformation, there is a slight left-handed twist which might suggest an unstable conformation prone to changing readily. We have even titrated the pH to as low as 3.2 (data not presented) and found no change in the conformation. However, it has been suggested that the pH of the endosome need not go below pH 5.0 for translocation of the LC (*25*). It is suggested that the HC−LC complex ingrained in the membrane acts like a chaperone.

The above results raise two questions. (1) Could a change in conformation due to pH be studied by crystal structure determination where packing forces of the crystal lattice might play a major role? Such studies have been carried out. Bullogh et al. (*43*) have shown that a peptide region changes

FIGURE 3: Ribbons representation of BoNT/B at pH 6.0. The three metal ions are shown as sphere models, zinc in gray and calcium in black. This figure was prepared with Molscript (*52*).

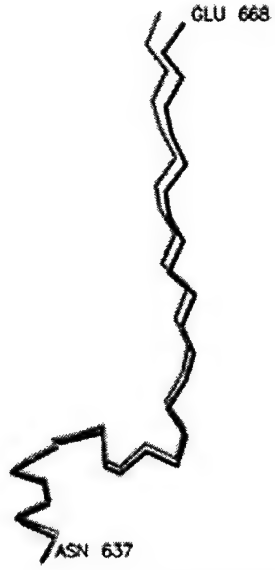

FIGURE 4: Putative transmembrane region of botulinum neurotoxin B. The α-C trace from structures determined at pH 4.0 (black) and 7.0 (gray) are superimposed, and no major change in conformation is seen. Conformations of this region at other pH values are similar and closer to that at pH 4.0.

its conformation drastically by determining the structures at two vastly different pHs. (2) If it is not the pH, what is responsible for the presumed change in conformation? This study cannot answer that question but can only show that something more than a reduction of the pH is required. Further studies such as the effect of lipids, phosphorylation of toxins, etc., need to be pursued.

Effect of pH on the Catalytic Domain and the Active Site Zinc. Li et al. (*44*) have reported that the zinc ion stays bound to the protein at a pH as low as 4.7. In our structure determination, we monitored the change in the overall conformation of the light chain, the presence of zinc, and specific changes in side chain conformations especially near the active site. As the pH is decreased from pH 6 to 4.0, it is found that the zinc ion gradually becomes disordered (as judged by the thermal factor) and finally is removed altogether. The thermal factor steadily increases compared to the average *B* factor of the protein atoms. Also, the thermal

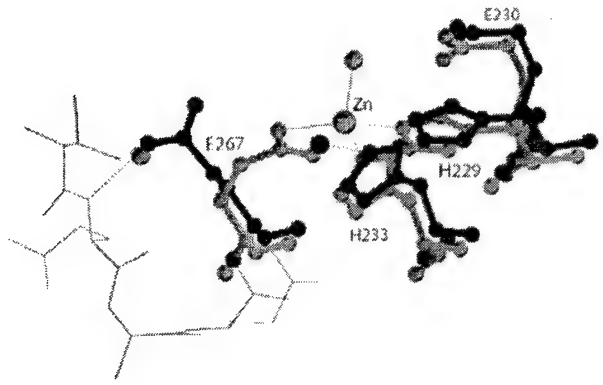

FIGURE 5: Active site of botulinum neurotoxin at pH 6.0 (green) and 4.0 (blue). At pH 6.0 and 7.0 (not shown), the side chain carboxylate oxygen coordinates with zinc. At pH 4.0, this coordination is lost and it takes a different rotamer position making a hydrogen bond with Gln264 (shown with a dashed line) and replaces a water molecule present at pH 6.0 (shown in green). Interestingly, a water molecule (shown in blue) replaces one of the original carboxylate oxygens. At pH 5.5, the side chain of Glu267 takes two discrete orientations. Also, at pH <5.0, the nucleophilic water is not seen in the electron density map.

factors of the terminal atoms of Glu267 increase, and the side chain becomes disordered. At pH 5.5, the side chain has two disordered positions. The position with the higher occupancy still maintains coordination with the zinc ion, while in the second orientation, the carboxylate group makes a hydrogen bond with the main chain nitrogen of Gln264. At pH 5.0, the side chain of Glu267 takes a completely new rotamer position and the coordination to zinc is lost and corresponds to the second disordered position at pH 5.5. Though the thermal factor of zinc increases, electron density persists for the zinc atom, in agreement with the published results (*44*). However, at pH 4.0 and 3.2, Glu267 takes the new rotamer position and there is no electron density for the zinc ion, suggesting that it has been removed completely. In structures at pH <5.0, the nucleophilic water is not present, whereas it is intact (though slightly moved) in structures at pH >5.0 (Figure 5). In all cases, there is no change in the overall conformation and the helical content remains constant contrary to results from biophysical studies which may be due to the difference in solid and solution states or the experimental conditions that are used.

Belt Region versus pH Variation. The main difference between the crystal structures of BoNT/A and BoNT/B (amino acids 481−530) is in the conformation of the belt region with respect to the active site. While the active site is shielded by the belt region in BoNT/A, it is almost completely open to the solvent region in BoNT/B. This difference was thought to be due to the difference in crystallization conditions (BoNT/A at pH 7 and BoNT/B at pH 6). While the zinc coordination remains the same as in the case of the pH 6.0 structure, there is no visible movement of the belt region, suggesting the difference may be real and serotype-specific (Figure 6). This will be confirmed only when structures of other serotypes become available.

Structure of Apo-BoNT/B. The crystal structure of BoNT/B crystallized after treatment with EDTA has been determined to 2.6 Å resolution. The apo-BoNT/B molecule closely resembles those at pH 4 and 3.2. There is no major change in the tertiary structure, and the rmsd is 0.813 Å when compared to the structure at pH 6 for 1270 α-C atoms. The Glu267 side chain takes a new rotamer position as at pH 4. Glu267 does not show any sign of disorder on the basis of its thermal factor, which is comparable to the average *B* value of the protein atoms. While a water molecule was found near the original position of Glu267 OE2 at pH 4, it is not present in the apo structure. This may possibly be due to the lower-resolution data of the apotoxin structure. There is a water molecule near the original zinc atom position (~1.4 Å away). This water molecule makes hydrogen bonds with His229 NE2 and His233 NE2 with distances 3.57 and 3.0 Å, respectively, but makes no hydrogen bond contacts with Glu230. The density for this water molecule appears to be elongated, and it could be disordered and might partially occupy the position corresponding to the original nucleophilic water molecule (Figure 1).

Role of Zinc in Botulinum Neurotoxins. The role of zinc in proteins could be either structural, functional, or both. In general, a catalytic zinc is coordinated to three amino acid residues and an activated water molecule (nucleophilic water). A structural zinc will be coordinated to four amino acid residues (*16*, *17*). In botulinum neurotoxins, classified

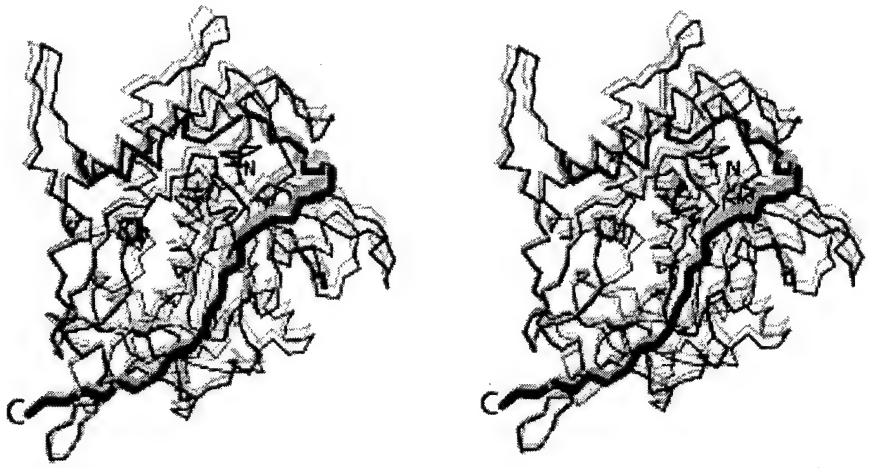

FIGURE 6: Superposition of α-C chains at pH 6.0 (gray) and 7.0 (black). The orientation of the belt region remains the same at all pH values and shows that in all cases the active site cavity is exposed and accessible to substrates. The belt region over the cavity is shown in thicker lines than the rest of the molecule.

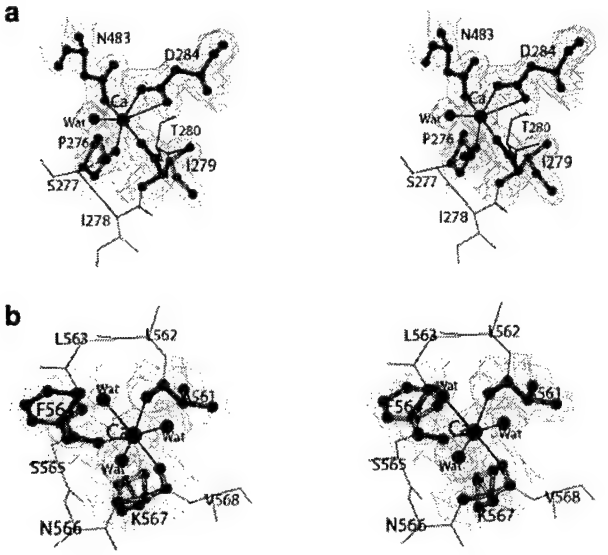

FIGURE 7: SigmaA-weighted $2F_o - F_c$ maps with the final Ca^{2+} positions superimposed: (a) calcium 1293 and (b) calcium 1294. Contours are drawn at the 1σ level.

as gluzincins, the zinc atom is coordinated with three amino acid residues and one water and is thought to be catalytic (*18*). It has been reported that the removal of zinc is reversible in botulinum neurotoxins while the catalytic activity is not. This led to the belief that the tertiary structure of the protein changes irreversibly when the zinc is removed (*21*). However, it has also been shown that zinc-depleted toxins can reach the cytosol and could be active since they could be reconstituted with zinc present in cytosol, which implies that there is no change in the conformation (*23*).

The presumed change in the tertiary structure was studied by biophysical methods (UV circular dichroism in BoNT/A). While no change in the conformation of tyrosine residues was observed, there were indications about the conformational change for phenylalanine residues. In BoNT/B, there are three phenylalanine residues in the light chain (194, 202, and 220). The α-C atoms of these residues are less than 16 Å from the zinc atom, but no change in their conformation or solvent accessibility is seen in either the holotoxin at pH 4.0 or apotoxin. However, for the BoNT/A light chain, the activity is reported to be partly restored when the protein is reconstituted with zinc. There are other reports which also suggest that the activity is restored. From our structural studies on the apotoxin, it is clear that removal of zinc does not affect the stability or conformation of the protein, and it could be concluded that its role is catalytic rather than structural. A similar role for active site zinc has also been proposed in carboxypeptidase (*45*).

Calcium Ions in Botulinum Neurotoxins. During the course of the high-resolution structural analysis, an interesting feature was discovered. Two strong peaks in the electron density map were observed which could not be ascribed to water molecules because of the relative peak heights and the comparatively short distance to the surrounding oxygens. They were identified as calcium ions and refined accordingly (Figure 7). The $F_o - F_c$ map with these two calcium ions included in the refinement showed no residual peak. One calcium ion is predominantly coordinated by light chain residues. It is coordinated by Pro276 O, Ile279 O, Asp284 OD1, Asp284 OD2, Asn483 ND2, and a water molecule (Table 2). While residues 276, 279, and 284 belong to the light chain, residue 483 belongs to the translocation domain and is in the beginning of the belt region. It is a slightly distorted octahedral coordination. The second calcium ion is entirely coordinated by the translocation domain and water molecules. It is coordinated by Ala561 O, Phe564 O, Lys567 O, and three water molecules which form a perfect octahedron (Figure 8 and Table 2). The coordination distances are in the range of 2.2−2.4 Å, values characteristic of calcium−oxygen contacts observed in calcium-containing

Table 2: Calcium Ion Coordination Distances

calcium	protein ligand	distance (Å)	calcium	protein ligand	distance (Å)
Ca 1293	Asp284 OD1	2.29	Ca 1294	Ala561 O	2.22
	Asp284 OD2	2.99		Phe564 O	2.24
	Pro276 O	2.39		Lys567 O	2.18
	Ile279 O	2.24		water 1349 O	2.18
	Asn483 ND2	2.26		water 1368 O	2.21
	water 1720 O	2.75		water 2018 O	2.41

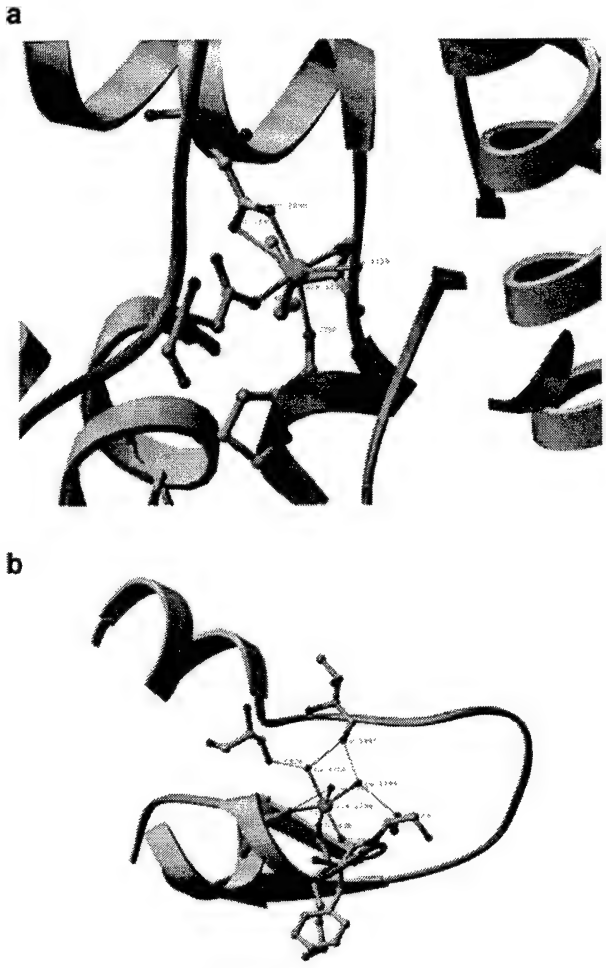

FIGURE 8: Coordination of calcium ions shown along with the secondary structure. (a) Calcium 1293 coordinates with Pro276, Ile279, Asp284, Asn483, and a water molecule and links the light chain and the belt region. This calcium ion may play a role in the translocation. (b) Calcium 1294 coordinates with Ala561, Phe564, Lys567, and three water molecules and is completely coordinated by residues in the translocation domain. This figure was prepared with Ribbons (*53*).

proteins (*46*−*48*). These interactions stabilize a knotlike loop (helix−β−helix). Ala561 and Lys567 (except in BoNT/A where it is Arg, a similarly charged residue) are conserved in all botulinum toxins and tetanus toxin. However, the coordination is through main chain oxygen atoms only. The two calcium ions have solvent accessibilities of 5 and 13 Å^2, and are almost buried.

Interestingly, in most of the zinc endopeptidases, calcium ions are present in addition to zinc. In thermolysin, four calcium ions are present and the thermal stability is attributed to these calcium ions (*48*, *49*). A calcium ion has also been identified in zinc endopeptidase adamalysin II and is thought to be important for structural stability (*47*). Calcium ions have not been identified so far in botulinum toxins by biochemical methods. However, in the initial spectroscopic experiments, only Zn, Co, Cu, Fe, Mn, and Ni were tested, not calcium. The activity of the zinc-depleted BoNT/A LC could be restored to ~20−30% of its original level by adding a divalent metal such as Mn, Mg, or Ca (*50*). Because of the nature of the binding site, it may have some functional role in addition to a structural role.

In the structures determined at various pHs, the calcium ions are intact and are not removed like zinc. This may be because the coordinating atoms are mostly main chain oxygens which are not protonated even at pH 3.0. However, in the apotoxin structure where the toxin was incubated with EDTA before crystallization, the two calcium ions are removed and are replaced with water molecules and the coordinating distances are increased to hydrogen bonding distances. The original calcium sites are perturbed, but no major change in the main chain fold is observed.

Role of Ca^{2+} in Biological Function. It is unknown if Ca^{2+} has a direct role in the biological activity of BoNTs. Ca^{2+} is not needed for catalytic activity, which proceeds unimpeded when BoNT was incubated with BAPTA prior to mixing with the solubilized SNAP-25 substrate (Figure 2a). To test the effect of Ca^{2+} on the catalytic activity of each serotype, BoNTs were added to neuronal cell lysates in the presence or absence of BAPTA or the zinc-specific chelator TPEN (*51*). BAPTA had no effect on the catalytic activity of either toxin (Figure 2a), whereas TPEN totally inhibited both BoNTs. We conclude that the two Ca^{2+} atoms do not influence light chain activity. To test if Ca^{2+} participates in the entry of toxin into cells, BoNT was applied to cultured neurons followed by the membrane-permeable BAPTA-AM or TPEN. These chelators were chosen because both are membrane-permeable, allowing both to act on intracellular BoNT. The amount of BoNT applied to cells was previously determined to cut approximately half of the total SNAP-25 or VAMP. BAPTA-AM effectively protected SNAP-25 and VAMP from BoNT/A and -B, respectively (Figure 2b). Furthermore, addition of Ca^{2+} 1 h after addition of either toxin restored BoNT activity, indicating that BAPTA-AM inhibits BoNT by removing Ca^{2+} (Figure 2c). Only a low-resolution crystal structure of BoNT/A is available, and accordingly, water molecules and other possible ions (except the active site zinc) have not been modeled. On the basis of the sequence homology and structural similarity of BoNT/A and BoNT/B, calcium ions will be present in BoNT/A and other *Clostridium* neurotoxins. Also, the coordination to calcium ion is mostly from main chain oxygen atoms in BoNT/B. A structural alignment of BoNT/A and -B reveals similar sequence homology at the calcium sites. Moreover, the electrostatic charge distribution is similar in BoNT/A and -B at the calcium site (data not shown).

Therefore, the results in living cells in combination with the cell-free SNARE cleavage assay demonstrate that neither Ca^{2+} atom contributes to catalytic activity but at least one Ca^{2+} atom is required for uptake of the toxin into neurons. Because addition of excess Ca^{2+} after toxin exposure reverses the BAPTA-AM effect in living cells, we presume Ca^{2+} is required for toxin activity after toxin uptake but before SNARE damage. Because Ca^{2+} is not required for toxin catalytic activity, we hypothesize that the Ca^{2+} atom coordinated by the light and heavy chains is required for either channel formation or LC translocation through the channel. The Ca^{2+} might allow the light chain to separate or change conformation as it enters the cytosol.

ACKNOWLEDGMENT

We thank Drs. A. Saxena and M. Becker for providing us beam time on the X12C and X25 beamlines of the National Synchrotron Light Source.

REFERENCES

1. Montecucco, C., and Schiavo, G. (1995) Structure and function of tetanus and botulinum neurotoxins, *Q. Rev. Biophys. 28*, 423−472.
2. Simpson, L. L. (1986) Molecular pharmacology of botulinum toxin and tetanus toxin, *Annu. Rev. Pharmacol. Toxicol. 26*, 427−453.
3. Schiavo, G., Matteoli, M., and Montecucco, C. (2000) Neurotoxins affecting neuroexocytosis, *Physiol. Rev. 80*, 717−766.
4. Schantz, E. J., and Johnson, E. A. (1992) Properties and use of botulinum toxin and other microbial neurotoxins in medicine, *Microbiol. Rev. 56*, 80−99.
5. Menestrina, G., Schiavo, G., and Montecucco, C. (1994) Molecular mechanisms of action of bacterial protein toxins, *Mol. Aspects Med. 15*, 79−193.
6. Oguma, K., Fujinaga, Y., and Inoue, K. (1995) Structure and Function of *Clostridium botulinum* toxins, *Microbiol. Immunol. 39*, 161−168.
7. Schiavo, G., Rossetto, O., Santucci, A., Dasgupta, B. R., and Montecucco, C. (1992) Botulinum neurotoxins are zinc proteins, *J. Biol. Chem. 267*, 23479−27483.
8. Blasi, J., Chapman, E. R., Link, E., Binz, T., Yamasaki, S., Camilli, P. D., Sudhof, T. C., Niemann, H., and Jahn, R. (1993) Botulinum neurotoxin A selectively cleaves the synaptic protein SNAP-25, *Nature 365*, 160−163.
9. Blasi, J., Chapman, E. R., Yamasaki, S., Binz, T., Niemann, H., and Jahn, R. (1993) Botulinum neurotoxin C blocks neurotransmitter release by means of cleaving HPC-1/syntaxin, *EMBO J. 12*, 4821−4828.
10. Binz, T., Blasi, J., Yamasaki, S., Baumeister, A., Link, E., Sudhof, T. C., Jahn, R., and Niemann, H. (1994) Proteolysis of SNAP-25 by Types E and A botulinum neurotoxins, *J. Biol. Chem. 269*, 1617−1620.
11. Schiavo, G., Shone, C. C., Rossetto, O., Alexander, F. C. G., and Montecucco, C. (1993) Botulinum neurotoxin serotype F is a zinc endopeptidase specific for VAMP/synaptobrevin, *J. Biol. Chem. 268*, 11516−11519.
12. Schiavo, G., Santucci, A., Dasgupta, B. R., Metha, P. P., Jontes, J., Benfenati, F., Wilson, M. C., and Montecucco, C. (1993) Botulinum neurotoxins serotypes A and E cleave SNAP-25 at distinct COOH-terminal peptide bonds, *FEBS Lett. 335*, 99−103.
13. Schiavo, G., Malizio, C., Trimble, W. S., Polverino-de-Laureto, P., Milan, G., Sugiyama, H., Johnson, E. A., and Montecucco, C. (1994) Botulinum G neurotoxin cleaves VAMP/synaptobrevin at a single Ala-Ala peptide bond, *J. Biol. Chem. 269*, 20213−20216.
14. Schiavo, G., Benfenati, F., Poulain, B., Rossetto, O., de-Lauretto, P. P., Dasgupta, B. R., and Montecucco, C. (1992) Tetanus and botulinum-B neurotoxins block neurotransmitter release by a proteolytic cleavage of synaptobrevin, *Nature 359*, 832−835.

15. Schiavo, G., Shone, C. C., Bennett, M. K., Scheller, R. H., and Montecucco, C. (1995) Botulinum neurotoxin type C cleaves a single Lys-Ala bond within the carboxyl-terminal region of syntaxins, *J. Biol. Chem. 270*, 10566−10570.
16. Vallee, B. L., and Auld, D. S. (1990) Zinc coordination, function, and structure of zinc enzymes and other proteins, *Biochemistry 29*, 5647−5659.
17. Vallee, B. L., and Auld, D. S. (1990) Active-site zinc ligands and activated H_2O of zinc enzymes, *Proc. Natl. Acad. Sci. U.S.A. 87*, 220−224.
18. Hooper, N. M. (1994) Families of zinc metalloproteases, *FEBS Lett. 354*, 1−6.
19. Foran, P., Shone, C. C., and Dolly, J. O. (1994) Differences in the protease activities of tetanus and botulinum B toxins revealed by the cleavage of vesicle-associated membrane protein and various sized fragments, *Biochemistry 33*, 15365−15374.
20. Fillippis, V. D., Vangelista, L., Schiavo, G., Tonello, F., and Montecucco, C. (1995) Structural studies on the zinc-endopeptidase light chain of tetanus neurotoxin, *Eur. J. Biochem. 229*, 61−69.
21. Fu, F., Lomneth, R. B., Cai, S., and Singh, B. R. (1998) Role of zinc in the structure and toxic activity of botulinum neurotoxin, *Biochemistry 37*, 5267−5278.
22. Li, L., and Singh, B. R. (2000) Role of zinc binding in type A botulinum neurotoxin light chain's toxic structure, *Biochemistry 39*, 10581−10586.
23. Simpson, L. L., Maksymowych, A. B., and Hao, S. (2001) The role of zinc binding in the biological activity of botulinum toxin, *J. Biol. Chem. 276*, 27034−27041.
24. Montecucco, C., Papini, E., and Schiavo, G. (1994) Bacterial protein toxins penetrate cells via a four-step mechanism, *FEBS Lett. 346*, 92−98.
25. Koriazova, L., and Montal, M. (2003) Translocation of botulinum neurotoxin light chain protease through the heavy chain channel, *Nat. Struct. Biol. 10*, 13−18.
26. Kadkhodayan, S., Knapp, M. S., Schmidt, J. J., Fabes, S. E., Rupp, B., and Balhorn, R. (2000) Cloning, expression, and one-step purification of the minimal essential domain of the light chain of botulinum neurotoxin type A, *Protein Expression Purif. 19*, 125−130.
27. Ransom, B. R., Neale, E., Henkart, M., Bullock, P. N., and Nelson, P. G. (1977) Mouse spinal cord in cell culture. I. Morphology and intrinsic neuronal electrophysiologic properties, *J. Neurophysiol. 40*, 1132−1150.
28. Fitzgerald, S. C. (1989) in *A Dissection and Tissue Culture Manual of the Nervous System* (Sharar, A., Devellis, J., Vernadakis, A., and Javer, B., Eds.) pp 219−222, Alan R. Liss, Inc., New York.
29. Williamson, L. C., Fitzgerald, S. C., and Neale, E. A. (1992) Differential effects of tetanus toxin on inhibitory and excitatory neurotransmitter release from mammalian spinal cord cells in culture, *J. Neurochem. 59*, 2148−2157.
30. Laemmli, U. K. (1970) Cleavage of structural proteins during the assembly of the head of bacteriophage T4, *Nature 227*, 680−685.
31. Li, L., Binz, T., Niemann, H., and Singh, B. R. (2000) Probing the mechanistic role of glutamate residues in the zinc-binding motif of type A botulinum neurotoxin light chain, *Biochemistry 39*, 2399−2405.
32. Swaminathan, S., and Eswaramoorthy, S. (2000) Structural analysis of the catalytic and binding sites of *Clostridium botulinum* neurotoxin B, *Nat. Struct. Biol. 7*, 693−699.
33. Swaminathan, S., and Eswaramoorthy, S. (2000) Crystallization and preliminary X-ray analysis of *Clostridium botulinum* neurotoxin type B, *Acta Crystallogr. D56*, 1024−1026.
34. Otwinowski, Z., and Minor, W. (1997) Processing of X-ray diffraction data collected in oscillation mode, *Methods Enzymol. 276*, 307−326.
35. Brunger, A. T., Adams, P. D., Clore, G. M., Delano, W. L., Gros, P., Grosse-Kunstleve, R. W., Jiang, J. S., Kuszewski, J., Nilges, M., Pannu, N. S., Read, R. J., Rice, L. M., Somonsom, T., and Warren, G. L. (1998) Crystallography and NMR system: a new software suite for macromolecular structure determination, *Acta Crystallogr. D54*, 905−921.
36. Jones, T. A., Zou, J., Cowtan, S., and Kjeldgaard, M. (1991) Improved methods in building protein models in electron density map and the location of errors in these models, *Acta Crystallogr. A47*, 110−119.
37. Furey, W., and Swaminathan, S. (1997) PHASES-95: A program package for the processing and analysis of diffraction data from macromolecules, *Methods Enzymol. 276*, 590−620.
38. Laskowski, R. A., MacArthur, M. W., Moss, D. S., and Thornton, J. M. (1993) PROCHECK: a program to check the stereochemical quality for assessing the accuracy of protein structures, *J. Appl. Crystallogr. 26*, 283−291.
39. Hoch, D. H., Romero-Mira, M., Ehrlich, B. E., Finkelstein, A., DasGupta, B. R., and Simpson, L. L. (1985) Channels formed by botulinum, tetanus, and diphtheria toxins in planar lipid bilayers: relevance to translocation of proteins across membranes, *Proc. Natl. Acad. Sci. U.S.A. 82*, 1692−1696.
40. Overly, C. C., Lee, K. D., Berthiaume, E., and Hollenbeck, P. J. (1995) Quantitative measurement of intraorganelle pH in the endosomal-lysosomal pathway in neurons by using ratiometric imaging with pyranine, *Proc. Natl. Acad. Sci. U.S.A. 92*, 3156−3160.
41. Persson, B., and Argos, P. (1996) Topology prediction of membrane proteins, *Protein Sci. 5*, 363−371.
42. Lacy, D. B., Tepp, W., Cohen, A. C., DasGupta, B. R., and Stevens, R. C. (1998) Crystal structure of botulinum neurotoxin type A and implications for toxicity, *Nat. Struct. Biol. 5*, 898−902.
43. Bullough, P. A., Hughson, F. M., Skehel, J. J., and Wiley, D. C. (1994) Structure of influenza haemagglutinin at the pH of membrane fusion, *Nature 371*, 37−43.
44. Li, L., and Singh, B. R. (2000) Spectroscopic analysis of pH-induced changes in the molecular features of type A botulinum neurotoxin light chain, *Biochemistry 39*, 6466−6474.
45. Greenblatt, H. M., Feinberg, H., Tucker, P. A., and Shoham, G. (1998) Carboxypeptidase A: Native, zinc-removed and mercury-replaced forms, *Acta Crystallogr. D54*, 289−305.
46. Bode, W., and Schwager, P. (1975) The refined crystal structure of bovine beta-trypsin at 1.8 Å resolution. II. Crystallographic refinement, calcium binding site, benzamidine binding site and active site at pH 7.0, *J. Mol. Biol. 98*, 693−717.
47. Gomis-Ruth, F. X., Kress, L. F., Kellermann, J., Mayr, I., Lee, X., Huber, R., and Bode, W. (1994) Refined 2.0 Å X-ray structure of the snake venom zinc endopeptidase adamalysin II, *J. Mol. Biol. 239*, 513−544.
48. Colman, P. M., Jansonius, J. N., and Matthews, B. W. (1972) The structure of thermolysin: an electron density map at 2−3 Å resolution, *J. Mol. Biol. 70*, 701−724.
49. Matthews, B. W., Weaver, L. H., and Kester, W. R. (1974) The conformation of thermolysin, *J. Biol. Chem. 249*, 8030−8044.
50. Ahmed, S. A., and Smith, L. A. (2000) Light chain of botulinum A neurotoxin expressed as an inclusion body from a synthetic gene is catalytically and functionally active, *J. Protein Chem. 19*, 475−487.
51. Simpson, L. L., Coffield, J. A., and Bakry, N. (1993) Chelation of zinc antagonizes the neuromuscular blocking properties of the seven serotypes of botulinum neurotoxin as well as tetanus toxin, *J. Pharmacol. Exp. Ther. 267*, 720−727.
52. Kraulis, P. J. (1991) MOLSCRIPT: a program to produce both detailed and schematic plots of proteins, *J. Appl. Crystallogr. 24*, 946−950.
53. Carson, M. (1991) Ribbons 2.0, *J. Appl. Crystallogr. 24*, 958−961.

BI035844K

Available online at www.sciencedirect.com
SCIENCE DIRECT®
Protein Expression and Purification 34 (2004) 95–102
Protein Expression & Purification
www.elsevier.com/locate/yprep

Cloning, high level expression, purification, and crystallization of the full length *Clostridium botulinum* neurotoxin type E light chain

Rakhi Agarwal, Subramaniam Eswaramoorthy, Desigan Kumaran, John J. Dunn, and Subramanyam Swaminathan*

Biology Department, Brookhaven National Laboratory, Upton, NY 11973, USA

Received 4 August 2003, and in revised form 14 October 2003

Abstract

The catalytic activity of the highly potent botulinum neurotoxins are confined to their N-terminal light chains (~50 kDa). A full-length light chain for the type E neurotoxin with a C-terminal 6× His-tag, BoNT/E-LC, has been cloned in a pET-9c vector and over-expressed in BL21 (DE3) cells. BoNT/E-LC was purified to homogeneity by affinity chromatography on Ni–NTA agarose followed by exclusion chromatography using a Superdex-75 sizing column. The purified protein has very good solubility and can be stored stably at −20 °C; however, it seems to undergo auto-proteolysis when stored at temperature ⩾4–10 °C. BoNT/E-LC is active on its natural substrate, the synaptosomal associated 25 kDa protein, SNAP-25, indicating that it retains a native-like conformation and therefore can be considered as a useful tool in studying the structure/function of the catalytic light chain. Recombinant BoNT/E-LC has been crystallized under five different conditions and at various pHs. Crystals diffract to better than 2.1 Å.

Keywords: Botulinum neurotoxin; Light chain; Cloning; Proteolytic activity; Auto-proteolytic; Crystallization

The seven antigenically distinct botulinum neurotoxins (BoNT/A–G)[1] produced by the anaerobic bacteria *Clostridium botulinum* are among the most potent bacterial protein toxins known [1]. They all share significant sequence homology, and structural and functional similarity and are released by autolysis as a protoxin. They cause flaccid paralysis by inhibiting acetylcholine release at the neuromuscular junction. In their active form they are composed of two polypeptide chains, a heavy (HC, 100 kDa) and a light chain (LC, 50 kDa), held together by a disulfide bond. The C-terminal half of the heavy chain mediates binding of the neurotoxin to specific neuronal receptors while the N-terminal half enables the catalytically active light chain to translocate into the cytosol [2].

All botulinum neurotoxin light chains (BoNT-LC) are metalloproteinases, which act by zinc dependent proteolysis of protein components involved in neurotransmitter exocytosis from presynaptic termini. They all contain a conserved zinc binding motif, HExxH + E, near the middle of their primary sequence and when active they contain at least one bound zinc atom, which has a major functional role in their catalytic mechanism [3,4]. Although they all share sequence and possibly structural similarity, each BoNT has exclusive substrate selectivity and scissile bond specificity [5]. For example, BoNT/A, /C, and /E cleave the synaptosomal associated 25 kDa protein, SNAP-25, [6–8] at different peptide bonds, while BoNT/B, /D, /F, and /G cleave the vesicle associated membrane protein VAMP, also known as synaptobrevin [9,10], but again each cuts at a different peptide bond. BoNT/C also cleaves syntaxin [5].

Though an experimental vaccine is available for botulism, no effective therapeutic treatment is yet available once symptoms appear, which is usually within 24 h after ingesting the toxin. To develop a structure-based drug to treat botulism victims, a high-resolution

* Corresponding author. Fax: 1-631-3443407.
E-mail address: swami@bnl.gov (S. Swaminathan).

[1] *Abbreviations used:* BoNT, botulinum neurotoxin; LC, light chain; GST, glutathione S transferase; SNAP-25, synaptosomal associated 25 kDa protein; VAMP, vesicle associated membrane protein.

1046-5928/$ - see front matter © 2003 Elsevier Inc. All rights reserved.
doi:10.1016/j.pep.2003.10.017

three-dimensional structure of BoNT-LC is a prerequisite. Crystal structures of BoNT/A, BoNT/B, BoNT/A-LC (unpublished results), and BoNT/B-LC are available [11–13]. Although the structures are similar, the specificity and selectivity of botulinum neurotoxins present a unique problem. If the structures are similar will the same drug act for all serotypes of botulinum neurotoxins? The active site conformation may be similar but there must be additional factors that define the substrate specificity. It is possible that the variation in sequence near the active site might present different environments for the substrate. Or, since the substrates for botulinum toxins are fairly large polypeptides, the binding sites may be different. To understand this, it is necessary to determine the three-dimensional structures of all serotypes or at least their light chains.

Large-scale crystallization trials typically require milligram amounts of a highly pure, soluble protein as starting material. Though expression and purification of full-length BoNT/E-LC have been reported [14,15], the low quantity of protein that was recovered ($\leqslant$1 mg/l) would require considerable scaleup to obtain sufficient material even to begin crystallization experiments. In this paper, we report the cloning of the full length BoNT/E–LC with a C-terminal 6× His-tag, in a pET-9c expression vector containing a bacteriophage T7 promoter. High-level expression and recovery of >30 mg of highly pure protein per liter of culture medium has been achieved. Conditions for protecting the protein from degradation while retaining enzymatic activity were determined. In addition, the preliminary results from crystallization experiments are also presented.

Materials and methods

Cloning of BoNT/E-LC gene

An ampicillin resistant inducible T5-promoter expression vector pBN17, encoding a full length (1263 bp) of botulinum neurotoxin E light chain (BoNT/E-LC) region fused to a C-terminal 6× His tag, was obtained from Dr. Thomas Binz, Medizinische Hochschule, Hanover, Germany. This plasmid was used as a template to amplify the light chain sequence with the His-tag using two primers (forward 5′-AGAAGATCT**CATATG**CCAAAAATTA ATAG-3′ and reverse 5′-TCT**GGATCC**AAGCTTAGG TTAGTGATGGTGATGGTGAT-3′) by polymerase chain reaction (PCR). These PCR primers were designed to possess the restriction sites at their 5′ ends (*Nde*I in the forward primer and *Bam*HI in the reverse primer, shown in bold), which were compatible with the pET-9c-vector multiple-cloning restriction sites. The PCRs were performed in 50 µl total volume containing pfu polymerase and its buffer (Stratagene), 0.2 mM of each dNTP, 20 pMol of both primers, and 200 ng pBN17 DNA. The samples were preheated for 2 min at 95 °C and then 35 cycles of PCR were performed: 20 s at 94 °C, 30 s at 55 °C, and 4 min at 68 °C. After the last cycle, the reaction was incubated for an additional 7 min at 68 °C. The PCR products were purified using the GFX columns (Amersham Biosciences) to remove excess primers and then digested with *Nde*I and *Bam*HI to generate cohesive ends for cloning into pET-9c. The digested products were purified by electrophoresis on a low melting point agarose gel and then ligated overnight to *Nde*I–*Bam*HI digested and dephosphorylated pET-9c DNA using the T4-ligation system (New England Biolabs). The ligated samples were electroporated into the *Escherichia coli* D1210 cells and plated onto the LB-agar–kanamycin plates. Several kanR colonies were picked and used to obtain plasmid DNAs, which were then checked for the presence of the correct DNA sequence for the entire BoNT/E-LC gene in both the strands by Big Dye terminator Cycle Sequencing (Applied Biosystems). One clone which showed the right sequence was selected for expression studies. The isolated plasmid LC-pET9c was transformed into chemically competent BL21 (DE3) cells. Out of several colonies obtained on the LB-kanamycin agar plates, a single colony, containing LC-pET-9c, was selected and grown for preparation of a glycerol freezer stock.

Expression and purification of his-tagged BoNT/E-LC protein

Five milliliters of 2× YT medium containing 100 µg/ml kanamycin was inoculated with 10 µl of the freezer stock of BL21 (DE3) cells containing LC-pET9c. After overnight growth at 37 °C, this culture was used to inoculate 500 ml of 2× YT + kanamycin medium in a 2 L flask and the cells were grown at 37 °C with shaking until the A_{600} reached 0.6. At this point, 1 mM IPTG was added to induce BoNT/E-LC expression and cells were incubated at 20 °C for an additional 12 h. The induced cells were harvested by centrifugation at 5000 rpm at 4 °C for 10 min. The cell pellet was resuspended in 20 ml lysis buffer (50 mM Na–phosphate, pH 8.0, 300 mM NaCl, 5 mM benzamidine, 0.5 mM PMSF, and 1 µg/ml pepstatin A) supplemented with two tablets of protease inhibitor cocktail (Roche) and 0.5 mg/ml lysozyme (Sigma), 2 ml Bugbuster (Novagen), and 6 mM iodoacetamide. The bacterial suspension was incubated at room temperature for 30 min to lyse cells. Two microliters of the Benzonase (Novagen) was added to the suspension to digest the DNA and reduce the viscosity of the lysate. After an additional 10 min, the lysate was centrifuged at 16,500 rpm for 30 min to remove the insoluble cell debris.

The supernatant obtained from the above step was allowed to mix with 5 ml Ni–NTA agarose, pre-equilibrated with phosphate buffer (50 mM Na–phosphate, pH 8.0, 300 mM NaCl), at 4 °C for an hour. The mixture

of Ni–NTA agarose and supernatant was poured into the glass column and the flow-through of the soluble fraction was collected. The column was washed with 75 ml of phosphate buffer followed by 10 ml washes with buffer containing 10, 20, and 50 mM imidazole. Tightly bound protein was eluted with 6 ml of 100 mM and 35 ml of 250 mM imidazole. Aliquots of all the above fractions were analyzed by electrophoresis on 4–20% Tris–Glycine SDS–PAGE gel followed by staining with Coomassie blue. A 50 kDa band corresponding to BoNT/E-LC reproducibly eluted in 100–250 mM imidazole fractions was obtained.

Recovery of BoNT/E-LC was calculated to be more than 30 mg/l of induced cell culture. At this stage it is nearly 80% pure. BoNT/E-LC was purified to >98% by gel filtration on a (2 × 20 in) column of Superdex-75. The protein was concentrated before loading onto the column by centrifuging at 5000 rpm using Centriprep YM-10, amicon filter (Millipore). This sizing column was also used to exchange the buffer from phosphate to 20 mM Hepes plus 200 mM NaCl. Fractions (2 ml) were collected and analyzed by SDS–PAGE. Peak fractions containing approximately 15 mg BoNT/E-LC were pooled from 500 ml induced culture and the protein was again concentrated to ~5.5 mg/ml using Centriprep YM-10. Further concentration of the protein has not been tried. However, the protein was fully soluble and stable at this concentration as no sign of precipitate was seen even after long time storage (>5 months) at 4–10 and −20 °C.

Expression and purification of GST-tagged SNAP-25 protein

A recombinant plasmid pGEX-2T encoding SNAP-25 protein (aa 1–206) with an N-terminal GST tag was kindly provided by Dr. Eric Johnson, University of Wisconsin. The GST-SNAP-25 fusion protein was expressed in BL21 cells and purified by affinity chromatography on a commercial GST-resin (Novagen) as per the user's manual and the protein was eluted from the column using reduced glutathione. The purification procedure was similar to the one described earlier for BoNT/E-LC. However, in this case no iodoacetamide was added to the lysis buffer.

Enzymatic activity of BoNT/E-LC

The proteolytic activity of BoNT/E-LC which was preserved at −20 °C was assayed in vitro using GST-SNAP-25 protein (49.7 kDa). The assay was performed in a final volume of 20 μl [20 mM Hepes, pH 7.4, 2 mM DTT, and 10 μM Zn $(CH_3COO)_2$], containing 0.5–100 nM concentrations of enzyme on 4–6 μM concentrations of the substrate GST-SNAP-25. The amounts of cleavage of GST-SNAP-25 (5 μM) by the light chain (5 nM) were determined by incubating the samples at 37 °C for 0, 1, 2, 3, 5, 10, 15, 30, 45, 60, 90, 120, and 180 min. The reactions were stopped by adding the 7 μl of 3× concentrated SDS–PAGE sample buffers which contains sufficient EDTA to chelate the Zn cofactor. The extent of cleavage was then evaluated following electrophoresis on 4–20% Tris–Glycine SDS–PAGE gels by the appearance and intensity of a new band at ~47 kDa due to the cleavage of the GST-SNAP-25 between aa 180 and 181.

Kinetics data were obtained by monitoring the amounts of GST-SNAP-25 proteolysis by the light chain (5 nM) at eight different concentrations of GST-SNAP-25, ranging from 5 to 90 μM, at a fixed time of incubation (15 min). The results were analyzed as described above followed by densitometry of the stained products using a PhosphorImager system (Alpha Imager 2200, Alpha Innotech, San Leandro, CA, USA).

Protein concentration and mass determination

The protein concentrations were determined initially by A_{278} reading on UV-Spectrophotometer (Perkin–Elmer) using a Quartz-cuvette of 1 cm path length. Later the concentrations were confirmed further and accurately quantitated using BCA (Pierce) Kit using bovine serum albumin (BSA) as a standard.

Molecular mass of the protein was determined to be 49,266 Da by the MALDI-MS with an Applied Voyager System 1192. The protein samples were suspended in sinapinic acid matrix and spotted onto the stainless steel plate. The conditions of the experiment were 25,000 V, guide wire voltage 0.27%, and the laser intensity 2051.

Crystallization of the BoNT/E-LC

The crystallization screening was carried out by the sitting drop vapor diffusion method using Hampton Research crystallization screens. Crystals were obtained in five different conditions using ammonium sulfate and/or PEG at various pHs ranging from 4.6 to 8.5 at room temperature. Diffraction quality crystals were obtained at room temperature using 0.5 M ammonium sulfate, 1.0 M Li_2SO_4, and 0.1 M Na–citrate trihydrate at pH 5.6 as precipitant and crystals grew to their full size in 2–6 days time.

Crystallographic data collection and analysis

X-ray diffraction data from native crystals were collected at the X12C beamline of the National Synchrotron Light Source, Brookhaven National Laboratory with Brandeis CCD based B4 detector. Crystals were briefly transferred to the mother liquor containing 20% glycerol and flash cooled in liquid nitrogen. The data were processed with *DENZO* and scaled and merged

with *SCALEPACK* [16]. Crystals diffracted to better than 2.1 Å resolution.

Results and discussion

Expression and purification of the full-length BoNT/E-LC

The gene of BoNT/E-LC with a C-terminal 6× His tag was initially present in the T5-promoter-based vector pBN17, and was transformed and expressed in the BL21 cells but the protein yield was less than 0.5 mg per liter of culture medium. In an attempt to get a higher yield, the gene was amplified by PCR and then was cloned into pET-9c, which is a bacteriophage T7-RNA polymerase promoter vector system. The T7-RNA polymerase is highly capable of transcribing almost any DNA linked to a T7 promoter [17]. The aim was to over-express the full-length light chain and maintain its catalytic activity.

The protein was over-expressed in BL21 (DE3) cells and the soluble fraction of the protein was allowed to selectively bind to Ni–NTA agarose through the His-tag. The protein was then eluted by increasing the imidazole concentration stepwise. The protein has been eluted largely in 100–250 mM imidazole concentrations (Fig. 1) and this suggested that the protein has been folded correctly and thus binds tightly to the column through the tail of His-tag. A major portion of the protein elution in the 250 mM fraction has also been reported by Kadkhodayan et al. [18] while working with BoNT/A-LC though the protein was deemed not folded properly since it could not cleave SNAP-25. But the BoNT/E-LC protein purified in this study from 250 mM fraction showed an extremely good proteolytic activity suggesting proper folding of the protein. However, BoNT/E-LC is a full-length protein while rBoNT/A-LC is a truncated version (devoid of 8 N-terminal and 32 C-terminal residues), which might contribute to this difference in activity. The C-terminal region is probably involved in forming a proper active/binding site conformation.

After Ni–NTA agarose column purification, the protein was purified further to more than 98% by using Superdex-75 column (Fig. 2). This step also helped in exchanging the buffer of the protein from phosphate to Hepes (20 mM Hepes, pH 7.4, 200 mM NaCl). This protein has been found to be very soluble (>5 mg/ml) in Hepes buffer.

Improvement of lysis buffer for increased protein solubility and decreased non-specific aggregation

The lysis buffer which was tried initially contained 50 mM Na phosphate, pH 8.0, 300 mM NaCl, 5 mM benzamidine, 0.5 mM PMSF, 1 μg/ml pepstatin A, two tablets of protease inhibitor cocktail (Roche), and 0.5 mg/ml lysozyme (Sigma), but during purification through Ni–NTA column, a significant amount of precipitation appeared in the 250 mM imidazole fraction immediately after the elution and only 8–10 mg protein could be purified from 1-L cell culture. Also, this protein could not be crystallized. In our modified procedure, commercially available Bugbuster (Novagen) was used and iodoacetamide was added. This helped in increasing the yield of protein to >4-fold and in decreasing the

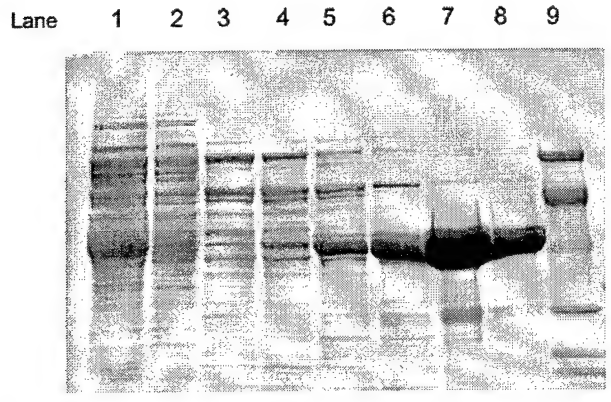

Fig. 1. Purification of BoNT/E-LC on a Ni–NTA agarose affinity column. The separated protein fractions were run on 4–20% Tris–Glycine SDS–PAGE gel and stained with Coomassie blue stain. Lane 1, supernatant/soluble fraction after lysis of cells; lane 2, flowthrough after Ni-chelation of supernatant; lane 3, 10 mM wash fraction; lane 4, 20 mM wash fraction; lane 5, 50 mM wash fraction; lane 6, 100 mM imidazole protein eluant; lanes 7–8, 250 mM imidazole protein eluant fractions; and lane 9, protein molecular weight marker.

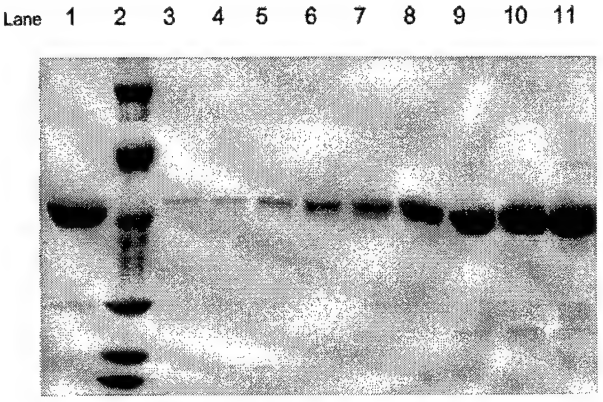

Fig. 2. Further purification of Ni–NTA affinity column purified BoNT/E-LC by Superdex-75 column. The separated fractions of protein have been electrophoresed in 4–20% Tris–Glycine SDS–PAGE and stained with Coomassie blue stain. Lane 1, Ni–NTA affinity column purified protein; lane 2, Protein molecular weight marker; and lanes 3–11, various fractions of protein separated through Superdex-75 column where probability of presence of protein was shown by the printed graph attached to column detector. Fractions 3–10 were pooled together and concentrated to 5.5 mg/ml.

precipitation of protein during purification. The protein was pure enough for crystallization trials. Probably the Bugbuster which contains a mixture of detergents helps in solubilizing the protein and iodoacetamide helps in reducing the non-specific aggregate formation by covalently modifying the free SH-group of cysteine residues of the protein. In a similar procedure, iodoacetamide and iodoacetate have been added during expression of BoNT/E-LC and purification of BoNT/B-LC, respectively [13,15].

Temperature and time dependent cleavage of BoNT/E-LC

The purified protein in Hepes buffer was stored at two different temperatures (−20 and 4–10 °C) to test the stability of the protein and the self-proteolysis reported by Ahmed et al. [19]. Both proteins were aliquoted and SDS–PAGE buffer was added to stop proteolysis in one tube at a time at increasing time intervals. The protein stored at −20 °C was stable even after five months and no self-proteolysis was observed. However, the protein stored at 4–10 °C showed on SDS–PAGE that the intensity of protein band corresponding to full-length protein (49 kDa) gradually diminishes with time while a new band corresponding to ~47 kDa emerges with increasing intensity with time (Fig. 3). After 2–3 weeks of storage, majority of protein was reduced to a ~47 kDa protein. This suggested a possible digestion of ~2 kDa protein from either C or N-terminus. Ahmed et al. [19] have reported a similar observation of cleavage in BoNT/A-LC from the C-terminal end. Although in the present case further major digestion and cleavage of the protein has not been seen even after long-time storage. The protein preserved at 4 °C was again allowed to bind to the Ni–NTA resin and centrifuged at 5000 rpm and the supernatant was checked by SDS–PAGE. It showed no band corresponding to the protein (either 47 or 49 kDa; data not shown). Since the His tag is at the C-terminus it is evident the protein must have bound to the nickel column and the cleavage must be near the N-terminus, unlike BoNT/A-LC.

However, appearance of a very faint band of 29–30 kDa is observed after 2–3 weeks of storage at 4 °C in the present case. But this could not be assumed as a major digestion of the protein, as majority of protein was still present as ~47 kDa protein in samples stored at 4 °C for 2–3 weeks. Both the above-mentioned cleavages were not observed in the samples stored at −20 °C. DasGupta and Foley [20] have also reported the fragmentation of the light chain isolated from the holotoxin to 2 fragments after 27 and 74 days but they have not mentioned any cleavage of ~2 kDa protein. Differences in results raise the question whether the native light chain isolated from holoprotein and the recombinant light chain may have the differences in fragmentation with respect to ~2 kDa cleavage?

Since we have used protease inhibitors extensively throughout the purification process, the presence of active trypsin like host proteolytic enzymes in our preparations seems highly unlikely. Most likely the protein is self-proteolytic like BoNT/A-LC since the digestion occurs at the same place in all preparations. However, the best condition to preserve the full length and high catalytic activity of the protein is to store it at or below freezing temperatures, i.e., −20 °C in Hepes buffer with or without 10–20% glycerol. This protein is also found to be stable in many freeze and thawing processes.

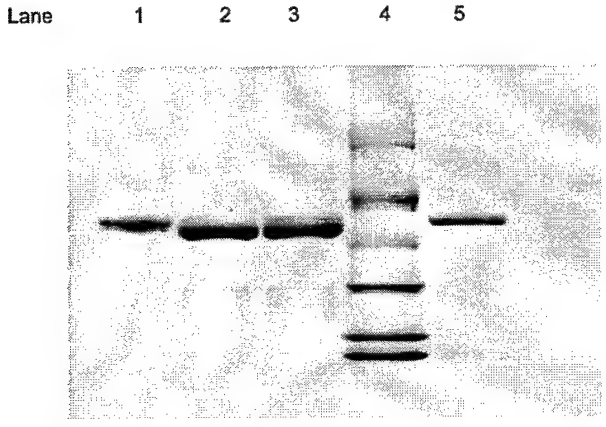

Fig. 3. The cleavage of BoNT/E-LC (~2 kDa) with time on storage at/or nearly 4–10 °C. Lanes 1–3, 1, 2, and 3-week-old samples stored at 4 °C, respectively; lane 4, protein molecular weight marker; and lane 5, 3-week-old protein sample preserved at −20 °C.

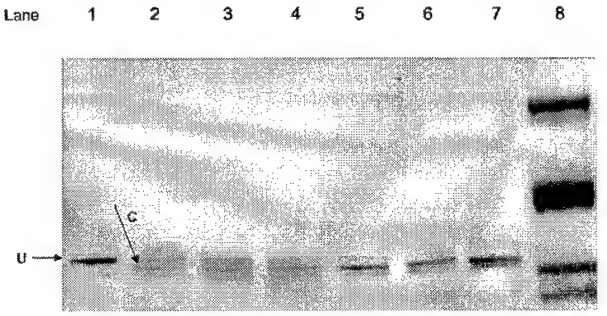

Fig. 4. The recombinant BoNT/E-LC is a catalytically active protein and cleaves efficiently its substrate SNAP-25. The protein reactions were performed with 5 nM concentration of BoNT/E-LC and 5 μM SNAP-25 at 37 °C. The samples were incubated for different time intervals and then reaction was stopped using the SDS-sample buffer. Lanes 1–7, reaction stopped after incubation at time 0, 1, 2, 3, 5, 10, and 15 min (reactions with longer incubation not shown in the figure). Lane 8, protein molecular weight marker. The proteins were separated on 4–20% Tris–Glycine SDS–PAGE gel and stained with Coomassie blue stain. U and C correspond to uncleaved and cleaved SNAP-25. A minor band below the cleaved band is due to impurity in SNAP-25 protein.

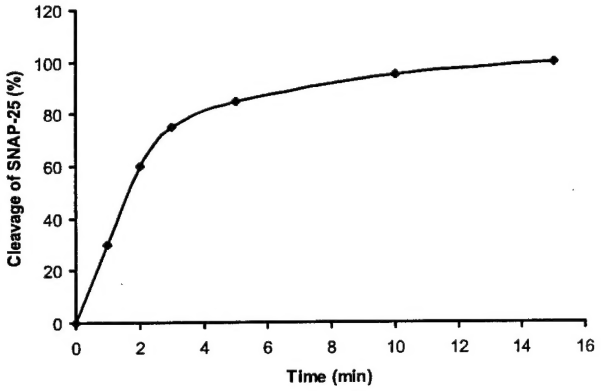

Fig. 5. The recombinant BoNT/E-LC catalytic activity graph showing time of incubation vs. percentage of substrate cleavage. The substrate concentration is 5 μM against 5 nm BoNT/E-LC.

Table 1
The kinetic values for SNAP-25 cleavage by BoNT/E-LC

K_m (μM)	V_{max} (μmol/min)	k_{cat} (s^{-1})	k_{cat}/K_m (mM^{-1}/s^{-1})
37.5	3.33	11.1	296

Catalytic activity of BoNT/E-LC

The 49.7 kDa SNAP-25 with the GST tag (GST-SNAP25) has been expressed and purified to 1.5–2.0 mg/100 ml of the cell culture. Purified GST-SNAP25 was used to monitor enzymatic activity of the BoNT/E-LC (stored at −20 °C for more than 42 days) on its native substrate since the presence of GST in the fusion protein GST-SNAP-25 does not interfere with the catalytic activity of botulinum neurotoxins [21,22]. This method of analysis used was similar to that reported by Blanes-Mira et al. [15].

Incubation of GST-SNAP-25 with BoNT/E-LC resulted in cleavage of peptide bond 180–181 of SNAP-25 and produced two fragments of sizes ~46.8 and ~2.9 kDa (the smaller fragment has migrated off the SDS gel in Fig. 4). The percentage cleavage of the substrate by enzyme at different time intervals (Fig. 5) showed that 5 nM light chain was able to completely cleave 5 μM SNAP-25 in 15 min of incubation at 37 °C. This suggests that the protein has a very high catalytic activity, which is comparable to the activity of the BoNT/E-LC reported by Blanes Mira et al. [15]. Additional experiments demonstrated that the digested GST-SNAP-25 protein can rebind to the GST resin, which is consistent with BoNT/E-LC cleavage within the C-terminal SNAP-25 portion of the fusion protein (presumably peptide bond 180–181 of SNAP-25).

The kinetic studies of cleavage results which were quantitated using the Phosphorimager System are summarized in Table 1.

Crystallization and preliminary crystallographic data analysis

The protein crystals were obtained in five different conditions at various pHs. Crystals were obtained in 2–6 days time and the best diffracting quality crystals were obtained using 0.5 M ammonium sulfate, 1.0 M Li_2SO_4,

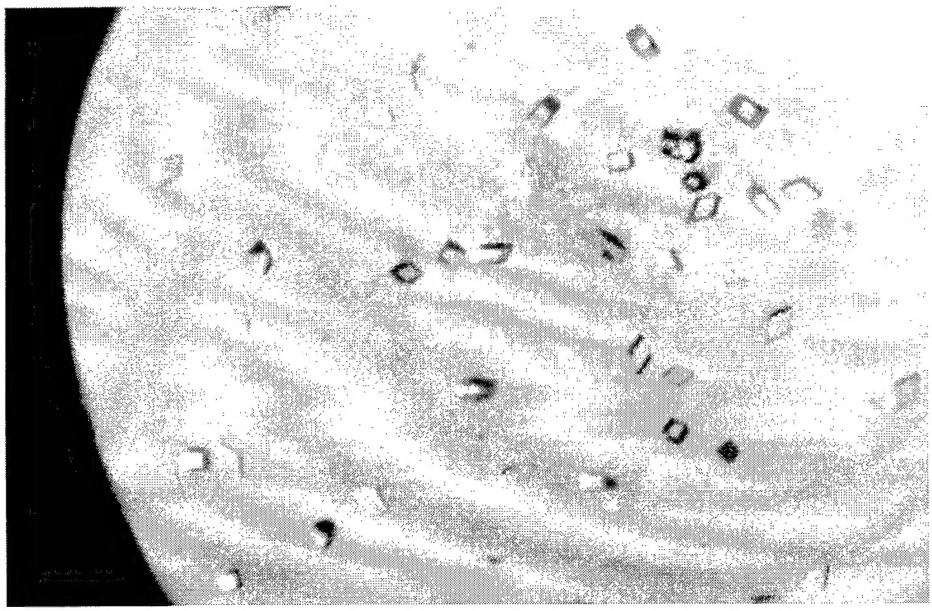

Fig. 6. Crystals of BoNT/E-LC. The average dimensions of the crystals are 0.3 × 0.3 × 0.2 mm. Crystals of different morphologies were also obtained (not shown in the figure).

and 0.1 M Na–citrate trihydrate at pH 5.6 as precipitant. Crystals attained their full growth within ten days (Fig. 6). These crystals diffract to better than 2.1 Å resolution. Crystals belong to the space group $P2_12_12$ with cell dimensions $a = 88.33$, $b = 144.45$, and $c = 83.37$ Å. Matthews coefficient was calculated to be 2.67 Da/Å^3 assuming two molecules per asymmetric unit. Preliminary X-ray diffraction data were collected at liquid nitrogen temperature at X12C beamline of National Synchrotron Light Source at Brookhaven National Laboratory (Table 2). A self-rotation function calculation with MolRep given in Fig. 7 shows the non-crystallographic 2-fold axis relating the two molecules in the asymmetric unit [23]. Initial attempts to solve the structure by the molecular replacement method using BoNT/B-LC or BoNT/A-LC as search model did not yield any solution. A heavy atom derivative search is in progress to determine the structure by the multiple isomorphous replacement method.

Table 2
Data collection statistics of recombinant BoNT/E-LC

Space group	P 2_12_12
a (Å)	88.33
b (Å)	144.45
c (Å)	83.37
Number of unique reflections	56,133
% Completion	98.1
Matthew coefficient V_m (Å/Da)	2.67
Solvent content (%)	55
# Molecules per asymmetric unit	2

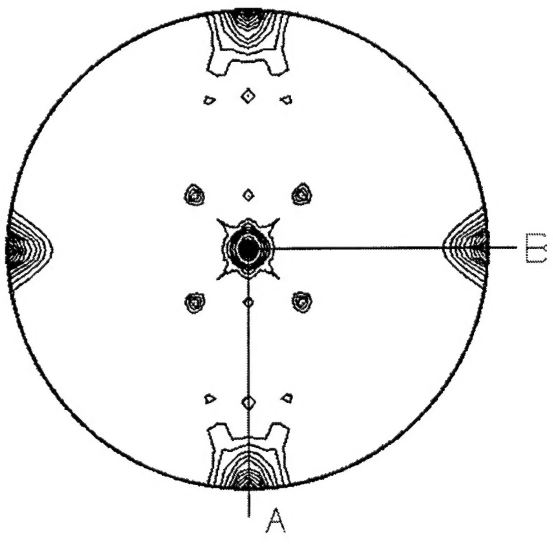

Fig. 7. $\kappa = 180°$ section of the stereographic projection of Patterson self-rotation function calculated with reflections in the resolution range 50–2.1 Å. The non-crystallographic 2-fold axis is seen at $\omega = 36°$ and $\phi = 45°$.

Acknowledgments

We thank Professor T. Binz for the recombinant clone for BoNT/E light chain and Dr. M. Bradshaw and Professor Eric Johnson for the recombinant clone for SNAP-25. We gratefully acknowledge a small grant provided by Allergan, USA. We also thank B. Lade for her technical assistance and help. Research was supported by the US Army Medical Research Institute of Infectious Diseases under US DOE Prime Contract No. DE-AC02-98CH10886 with Brookhaven National Laboratory.

References

[1] G. Schiavo, O. Rossetto, C. Montecucco, Clostridial neurotoxins as tools to investigate the molecular events of neurotransmitter release, Semin. Cell Biol. 5 (1994) 221–229.
[2] P. Foran, C.C. Shone, J.O. Dolly, Differences in the protease activities of tetanus and botulinum B toxins revealed by the cleavage of vesicle-associated membrane protein and various sized fragments, Biochemistry 33 (1994) 15365–15374.
[3] G. Schiavo, O. Rossetto, A. Santucci, B.R. Dasgupta, C. Montecucco, Botulinum neurotoxins are zinc proteins, J. Biol. Chem. 267 (1992) 23479–27483.
[4] G. Schiavo, O. Rossetto, F. Benfenati, B. Poulain, C. Montecucco, Tetanus and botulinum neurotoxins are zinc proteases specific for components of the neuroexocytosis apparatus, Ann. N. Y. Acad. Sci. 710 (1994) 65–75.
[5] G. Schiavo, M. Matteoli, C. Montecucco, Neurotoxins affecting neuroexocytosis, Physiol. Rev. 80 (2000) 717–766.
[6] G. Schiavo, A. Santucci, B.R. Dasgupta, P.P. Metha, J. Jontes, F. Benfenati, M.C. Wilson, C. Montecucco, Botulinum neurotoxins serotypes A and E cleave SNAP-25 at distinct COOH-terminal peptid bonds, FEBS Lett. 335 (1993) 99–103.
[7] T. Binz, J. Blasi, S. Yamasaki, A. Baumeister, E. LInk, T.C. Sudhof, R. Jahn, H. Niemann, Proteolysis of SNAP-25 by types E and A botulinum neurotoxins, J. Biol. Chem. 269 (1994) 1617–1620.
[8] L.C. Williamson, J.L. Halpern, C. Montecucco, J.E. Brown, E.A. Neale, Clostridial neurotoxins and substrate proteolysis in intact neurons: botulinum neurotoxin C acts on synaptosomal-associated protein of 25 kDa, J. Biol. Chem. 271 (1996) 7694–7699.
[9] C. Montecucco, G. Schiavo, Structure and function of tetanus and botulinum neurotoxins, Q. Rev. Biophys. 28 (1995) 423–472.
[10] G. Schiavo, C. Malizio, W.S. Trimble, P. Polverino-de-Laureto, G. Milan, H. Sugiyama, E.A. Johnson, C. Montecucco, Botulinum G neurotoxin cleaves VAMP/synaptobrevin at a single Ala–Ala peptid bond, J. Biol. Chem. 269 (1994) 20213–20216.
[11] D.B. Lacy, W. Tepp, A.C. Cohen, B.R. DasGupta, R.C. Stevens, Crystal structure of botulinum neurotoxin type A and implications for toxicity, Nat. Struct. Biol. 5 (1998) 898–902.
[12] S. Swaminathan, S. Eswaramoorthy, Structural analysis of the catalytic and binding sites of *Clostridium botulinum* neurotoxin B, Nat. Struct. Biol. 7 (2000) 693–699.
[13] M.A. Hanson, R.C. Stevens, Cocrystal structure of synaptobrevin-II bound to botulinum neurotoxin type B at 2.0 Å resolution, Nat. Struct. Biol. 7 (2000) 687–692.
[14] V.V. Vaidyanathan, K.-i. Yoshino, M. Jahnz, C. Dorries, S. Bade, S. Nauenburg, H. Niemann, T. Binz, Proteolysis of SNAP-25 isoforms by botulinum neurotoxin types A, C, and E: domains and amino acid residues controlling the formation of enzyme–substrate complexes and cleavage, J. Neurochem. 72 (1999) 327–337.
[15] C. B-Mira, C. Ibanez, G. F-Ballester, R. P-Cases, E. P-Paya, A. F-Montiel, Thermal stabilization of the catalytic domain of

botulinum neurotoxin E by phosphorylation of a single tyrosine, Biochemistry 40 (2001) 2234–2242.

[16] Z. Otwinowski, W. Minor, Processing of X-ray diffraction data collected in oscillation mode, Methods Enzymol. 276 (1997) 307–326.

[17] F.W. Studier, A.H. Rosenberg, J.J. Dunn, J.W. Dubendorff, Use of T7 RNA polymerase to direct expression of cloned genes, Methods Enzymol. 185 (1990) 60–89.

[18] S. Kadkhodayan, M.S. Knapp, J.J. Schmidt, S.E. Fabes, B. Rupp, R. Balhorn, Cloning, expression, and one-step purification of the minimal essential domain of the light chain of botulinum neurotoxin type A, Protein Expr. Purif. 19 (2000) 125–130.

[19] S.A. Ahmed, L.A. Smith, Light chain of botulinum A neurotoxin expressed as an inclusion body from a synthetic gene is catalytically and functionally active, J. Protein Chem. 19 (2000) 475–487.

[20] B.R. DasGupta, J. Foley, C. Botulinum, neurotoxin types A and E: isolated light chain breaks down into two fragments. Comparison of their amino acid sequences with tetanus neurotoxin, Biochemie 71 (1989) 1193–1200.

[21] P. Washbourne, R. Pellizzari, G. Baldini, M.C. Wilson, C. Montecucco, Botulinum neurotoxin A and E require the SNARE motiif in SNAP-25 for proteolysis, FEBS Lett. 418 (1997) 1–5.

[22] M. Rigoni, P. Caccin, E.A. Johnson, C. Montecucco, O. Rossetto, Site-directed mutagenesis identifies active-site residues of the light chain of botulinum neurotoxin type A, Biochem. Biophys. Res. Commun. 288 (2001) 1231–1237.

[23] A. Vagin, A. Teplyakov, An approach to multi-copy search in molecular replacement, Acta Crystallogr. D 56 (2000) 1622–1624.

APPENDIX 3

CRYSTAL STRUCTURE OF THE BINDING DOMAIN OF TETANUS TOXIN: DISIALYLLACTOSE COMPLEX

S. Jayaraman, S. Eswaramoorthy, D. Kumaran, & S. Swaminathan, Biology Department, Brookhaven National Laboratory, Upton, NY 11973, USA

Clostridium neurotoxins comprise of botulinum (BoNT) and tetanus neurotoxins (TeNT) and both cause neuronal disorder. BoNTs act at the presynaptic membranes while TeNT acts at the central nervous system. They share significant sequence and functional similarity and are expected to have similar three-dimensional structures. The active *C.* neurotoxins are dichains, a 100 kDa C-terminal heavy chain (HC) and a 50 kDa N-terminal light chain (LC). The HC has two functional domains, a binding domain and a translocation domain. The binding domain binds to gangliosides on the surface of the presynaptic membranes and it has been shown that *C.* neurotoxins bind to GT1b. Here we present the crystal structure of the binding domain of tetanus neurotoxin complexed with disialyllactose which is the head sugar group of GD3. The structure of the complex has been determined to a resolution of 2.3 Å. X-ray diffraction data were collected at the liquid nitrogen temperature at the National Synchrotron Light Source, Brookhaven National Laboratory. The structure was solved by the molecular replacement method. The sugar molecule was identified from the difference Fourier map and the structure was refined using CNS. Interestingly disialyllactose forms one branch of the sugar molecule of GT1b. Results from this study in conjunction with our previous studies will be used to model GT1b binding to *C.* neurotoxins.